RECORDING HEAD FLYING HEIGHT MEASUREMENT USING PHASE COMPARISON MICHELSON INTERFEROMETRY

TEPPARIT TANOI

A THESIS SUBMITED IN A PARTIAL FULFILMENT

OF THE REQUIREMENT FOR THE DEGREE OF

MASTER OF ENGINEERING IN DATA STORAGE TECHNOLOGY

COLLEGE OF DATA STORAGE INNOVATION

KING MONGKUT'S INSTITUTE OF TECHNOLOGY LADKRABANG

2013

KMITL-2013-DS-M-001-02

วิทยาลัยนวัตกรรมการจัดการข้อมูล
สถาบันเทคโนโลยีพระจอมเกล้าเจ้าคุณทหารลาดกระบัง
ใบรับรองวิทยานิพนธ์

หัวข้อวิทยานิพนธ์	การวัดระยะการบินของหัวอ่านเขียนโดยใช้วิธีการเฟสคอมแพริซันไมเคิลสันอินเตอร์เฟอร์โรมิเตอร์
Thesis Title	RECORDING HEAD FLYING HEIGHT MEASUREMENT USING PHASE COMPARISON MICHELSON INTERFEROMETRY
นักศึกษา	นายเทพฤทธิ์ ทาน้อย
รหัสประจำตัว	51068915
ปริญญา	วิศวกรรมศาสตรมหาบัณฑิต
สาขาวิชา	เทคโนโลยีการบันทึกข้อมูล
อาจารย์ที่ปรึกษาวิทยานิพนธ์	ผู้ช่วยศาสตราจารย์ ดร.ศิริเดช บุญแสง
หมายเลขวิทยานิพนธ์	KMITL-2013-DS-M-001-02

คณะกรรมการสอบวิทยานิพนธ์		ลายมือชื่อ
ผู้ช่วยศาสตราจารย์ ดร.สมยศ	เกียรติวนิชชัย	
ผู้ช่วยศาสตราจารย์ ดร.ศิริเดช	บุญแสง	
ดร.อนรรฆพล	แสนพิน	
ดร.ราชศักดิ์	ศักดาวิทิตกุล	
รองศาสตราจารย์ ดร.วันชัย	โพจิตโรจนา	

วัน/เดือน/ปี ที่สอบ 7 มีนาคม 2556 เวลา 10.30 - 12.30 น.
สถานที่สอบ อาคารเฉลิมพระเกียรติ 55 พรรษา สมเด็จพระเทพรัตนราชสุดาฯ สยามบรมราชกุมารี

วิทยาลัยนวัตกรรมการจัดการข้อมูล รับรองแล้ว

(รองศาสตราจารย์ ดร.อภินันท์ ธนชยานนท์)
คณบดี วิทยาลัยนวัตกรรมการจัดการข้อมูล

วันที่ 27 มีนาคม พ.ศ. 2556

หัวข้อวิทยานิพนธ์	การวัดระยะการบินของหัวอ่านเขียนโดยใช้วิธีการเฟสคอมแพริซันไมเคิลสันอินเตอร์เฟอร์โรมิเตอร์
นักศึกษา	นายเทพฤทธิ์ ทาน้อย
รหัสประจำตัว	51068915
ปริญญา	วิศวกรรมศาสตรมหาบัณฑิต
สาขาวิชา	เทคโนโลยีการบันทึกข้อมูล
พ.ศ.	2556
อาจารย์ที่ปรึกษาวิทยานิพนธ์	ผศ.ดร.ศิริเดช บุญแสง

บทคัดย่อ

พารามิเตอร์สำคัญที่มีผลต่อความจุของฮาร์ดดิสก์ คือ ระยะการบิน (Flying height) ของหัวอ่านเขียน วิธีการหนึ่งที่สามารถเพิ่มความจุในการเก็บข้อมูลของฮาร์ดดิสก์ทำได้โดยการลดระยะการบินของหัวอ่านเขียนให้น้อยกว่า10 นาโนเมตร ในปัจจุบันการวัดระยะการบินของหัวอ่านเขียนจะใช้วิธีอินเทนซิตี้อินเตอร์เฟอร์โรมิตรี (intensity interferometry) ซึ่งจะหาระยะการบิน (Flying height) ของหัวอ่านเขียนจากการคำนวณความเข้มของแสงที่เกิดจากการแทรกสอดระหว่างหัวอ่านเขียนและแผ่นบันทึกข้อมูล ซึ่งข้อจำกัดของวิธีนี้ คือ ความแม่นยำของเครื่องมือวัดจะลดลงที่ระยะน้อยกว่า 60 นาโนเมตร และเพื่อแก้ไขข้อจำกัดของวิธีนี้ จึงได้มีการนำเสนอวิธีเฟสคอมแพริซันไมเคิลสันอินเตอร์เฟอร์โรมิเตอร์ (Phase comparison Michelson interferometry (PCMI)) โดยการใช้เครื่องอินเตอร์เฟอร์โรเมตริกรีซีฟเวอร์วัดค่าเฟสและคำนวณเป็นระยะการบินของหัวอ่านเขียน

วิทยานิพนธ์ฉบับนี้ นำเสนอระบบวิธีการวัดระยะการบินของหัวอ่านเขียนด้วยวิธีการเฟสคอมแพริซันไมเคิลสันอินเตอร์เฟอร์โรมิเตอร์โดยการสร้างแบบจำลองการวัดระยะบินของหัวอ่านเขียน ซึ่งพัฒนาจากพื้นฐานของวิธีดูอัลบีมนอร์มอลอินซิเดนซ์โพลาไรเซชั่นอินเตอร์เฟอร์โรมิเตอร์ (Dual-beam normal incidence polarization interferometry) สร้างสัญญาณแทรกสอดซึ่งเป็นตัวแทนของระยะการบินของหัวอ่านเขียน และถูกบันทึกไว้ในรูปของสัญญาณแบบไม่ต่อเนื่องตามเวลา จากนั้นคำนวณหาค่าเฟสคอมแพเริซันโดยใช้ทฤษฎีฮิลเบิร์ททรานฟอร์ม (Hilbert transform) ในการคำนวณหาค่าเฟสและคำนวณเปรียบเทียบกลับมาเป็นระยะการบินซึ่งผลลัพธ์ของการคำนวณสัญญาณที่บันทึกได้แสดงให้เห็นว่าวิธีการเฟสคอมแพริซันไมเคิลสันอินเตอร์เฟอร์โรมิเตอร์ที่ใช้ทฤษฎีฮิลเบิร์ททรานฟอร์มในการคำนวณมีประสิทธิภาพในการวัดระยะการบินที่น้อยกว่า 10 นาโนเมตร ได้ไม่แตกต่างจากการใช้เครื่องอินเตอร์เฟอร์โรเมตริกรีซีฟเวอร์

Thesis	Recording Head Flying Height Measurement Using Phase Comparison Michelson Interferometry
Student	Mr.Tepparit Tanoi
Student ID.	51068915
Degree	Master of Engineering
Program	Data Storage Technology and Application
Year	2013
Thesis Advisor	Asst.Prof.Dr.Siridech Boonsang

ABSTRACT

The effective critical parameter in hard disk drive (HDD) is flying height. With increasing the recording density, head flying height has been minimized to sub 10 nanometers. Currently, intensity interferometryhas been implemented for measuring head flying height. The method is calculation of intensity of the interfered light reflected from the slider-disk interface. Butthe disadvantage of intensity interferometry is the sensitivity is reduced to half at below 60 nanometers and continues to worsen below this height. A novel method called phase comparison Michelson interferometry (PCMI) has been proposed to improve sensitivity and simplify the optical system.

This thesis presented a method for recording head flying height measurement using phase comparison Michelson interferometry. The proposed flying height measurement set is developed base on Dual-beam normal incidence polarization interferometry. The optical interferometry is used for capturing interference signal instead of interferometry receiver. The interference signal is captured and calculated by using a one-dimensional discrete Hilbert transform. The result indicated that the phase comparison Michelson interferometry with one-dimensional discrete Hilbert transform was achieved flying height measurement in sub 10 nanometers.

Acknowledgement

First of all, I would like to express my sincere thank fullness to Asst. Prof. Dr. Siridech Boonsang for his advice and encouragement while working on this thesis. I would like to express my gratitude to my boss, Mr. Weerayut Ngamsom and Mr. Wanna Yiemweth for being support of my education achievement and professional advancement. Finally, I would like to specially thank my family for their motivating and encouraging me during my studying in this thesis.

Tepparit Tanoi

Contents

Contents (Cont)

List of tables

List of figures

List of figures (Cont)

Figures **Pages**

Chapter 1

Introduction

1.1 Introduction

The amount of data that can be stored on a disk is a measurement of its areal recording density, i.e., the tracks per inch and the data bits per square inch. The product of these two is areal density in bits per square inch. Therefore, to increase areal density you must increase the number of bits on a track or the number of tracks per inch. Unfortunately, as the number of bits increases, the read signals generated by the bits weaken. This situation, in turn, makes it more difficult for the hard drive's read channel electronics to identify the bit patterns that re-create the user data.

The best way for read/write heads to maximize areal density is to reduce the distance from the head to the disk-the head's "fly height". A reduction in fly height makes the bit pattern's output signal stronger and easier to detect. The objective of reducing fly height is to improve the signal quality, and not create a condition that might damage stored data.

Head flying height is the most effective critical parameters in hard disk drive (HDD). With increasing the recording density, head flying height has been minimized to nanometer scale. Currently, a high precision system employing interferometry technique has been used for testing this parameter. To date, there are many methods to measure a nanometer spacing range such as multiple wavelength interferometry (MWI) [5]. The multiple wavelength interferometry (MWI) has been implemented in the well-known dynamic flying height tester (DFHT) but, with a limitation of the dynamic flying height tester are on accuracy and calibration issue. To achieve the measurement of nanometer scale spacing phase base interferometry has been introduced because of their high sensitivity and robust at any spacing range.

To improve accuracy and simplify the optical system of fly height measurement, a novel method has been introduced as called phase comparison Michelson interferometry (PCMI) [5], which is based on phase comparisons between two fringe patterns formed on slider and disk surfaces by Michelson interferometry. In this thesis we present a method for measuring phase difference using a one-dimensional discrete Hilbert transform for application in fly height tester.

1.2 Objectives

1. To setup an experiment of measuring the head flying height.
2. To measure head flying height using a phase difference measurement method.
3. To calculate the head flying height using a one-dimensional discrete Hilbert transform.

1.3 Outcomes and Expectation

From this studying we expect that the result can be developed the method of head flying height measurement in hard disk drive by using a method for measuring phase difference using a one-dimensional discrete Hilbert transform.

1.4 Conceptual Framework

This thesis study on a method for measuring phase difference using a one-dimensional discrete Hilbert transform for spacing measurement based on the phase comparison of two kinds of interference fringe patterns formed on the experiment slider and disk surfaces along the sliding direction. Experiments are setup to validate the accuracy and reproducibility of phase comparison Michelson interferometry method, which is considered to be valid even for the sub-10 nm spacing range.

1.5 Hypothesis

Reader sensor resistance and signal amplitude of TMR head will significantly change and eventually break down due to the thermal effect from heater voltage and laser power and reader sensor resistance and signal amplitude are proportional to energy applied.

1.6 Scope of the Study

The research studies the head flying height measurement technique by a method for measuring phase difference using a one-dimensional discrete Hilbert transform. The result is focus on the space of gap between experiment disk and experiment slider only.

Chapter 2

Theory and Literature Review

The main purpose of this study of flying height measurement by capture the interference signal then calculating the phase difference and actual flying height using a one-dimensional discrete Hilbert transform.

Thus, the following theory is expected and reviewed in order to conceptualize the framework and the related theory for this study.

2.1 Flying Height

One distinguishing characteristic of hard disk technology that makes it different from how floppy disks, VCRs and tape decks work is that the read/write heads do not make contact with the media. The reason for this is that due to the high speed that the hard disk spins, and the need for the heads to frequently scan from side to side to different tracks, allowing the heads to contact the disk would result in unacceptable wear to both the delicate heads and the media. In fact the earliest hard disks did have their heads in contact with the media, and this design was changed due to the wear that contact caused.

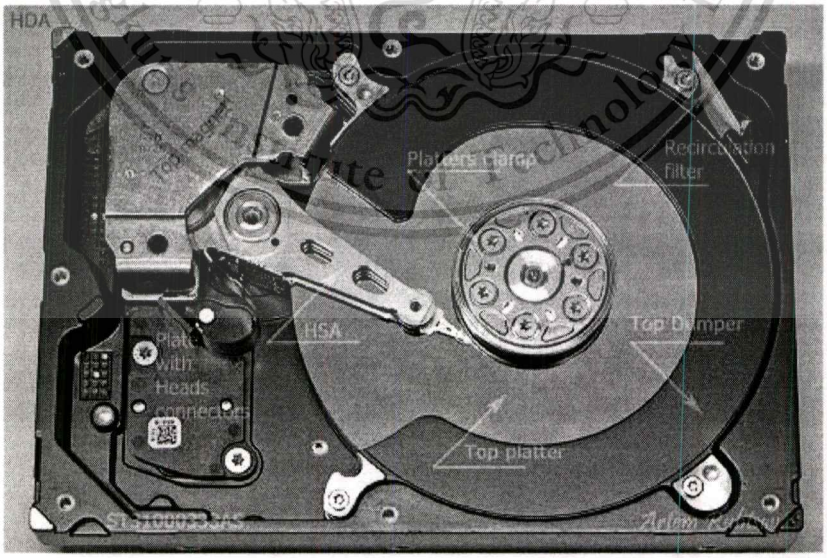

Figure 2.1 Hard disk drive (HDD)

http://hddscan.com/doc/HDD_from_inside.html

Modern drive heads float over the surface of the disk and do all of their work without

ever physically touching the platters they are magnetizing. The amount of space between the heads and the platters is called the floating height or flying height. It is also sometimes called the head gap, and some hard disk manufacturers refer to the heads as riding on an "air bearing". The read/write head assemblies are spring-loaded--using the spring steel of the head arms--which causes the sliders to press against the platters when the disk is stationary. (This is done to ensure that the heads don't drift away from the platters; maintaining an exact floating height is essential for correct operation.)

Figure 2.2 Head-Disk Interfaces

http://hddscan.com/doc/HDD_from_inside.html

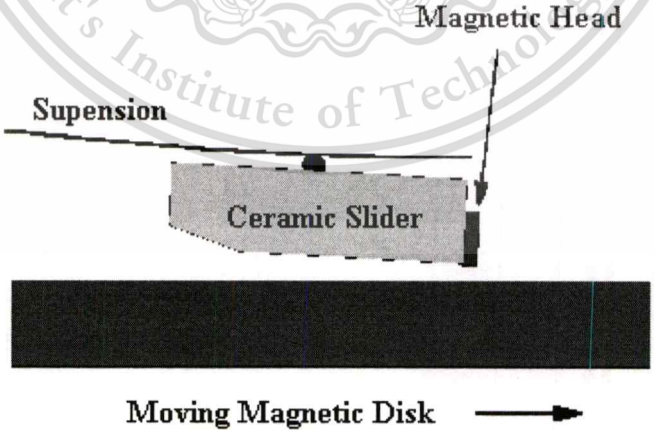

Figure 2.3 Head flying height

http://www.dataclinic.co.uk/data-recovery/hard-disk-functionality.htm

When the disk spins up to operating speed, the high speed causes air to flow under the sliders and lift them off the surface of the disk, the same principle of lift that operates on aircraft wings and enables them to fly.

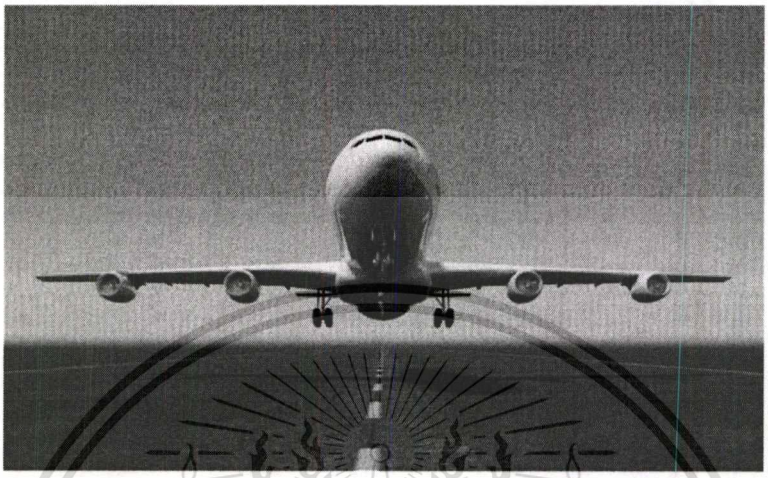

Figure 2.4 Head flying height, the same principle of lift that operates on aircraft wings http://www.cbc.ca/news/pointofview/2010/02/

Due to the very small distance from the heads to the plattersnormally measured in billions of an inch. The hard disk is assembled in a clean room containing air specially filtered to remove all the tiniest particles. Air however is required for the heads to function. The disk's internal environment is separate from the outside air to keep it clean; air exchange is permitted between the outside and inside of the drive to allow the drive to adjust to changes in air pressure. A special "breather" filter is installed to prevent foreign matter from contaminating the drive. If a drive is used at too high an altitude, the air will become too thin to support the heads at their proper operating height and failure will result; special industrial drives that truly are sealed from the outside are made for these special applications.

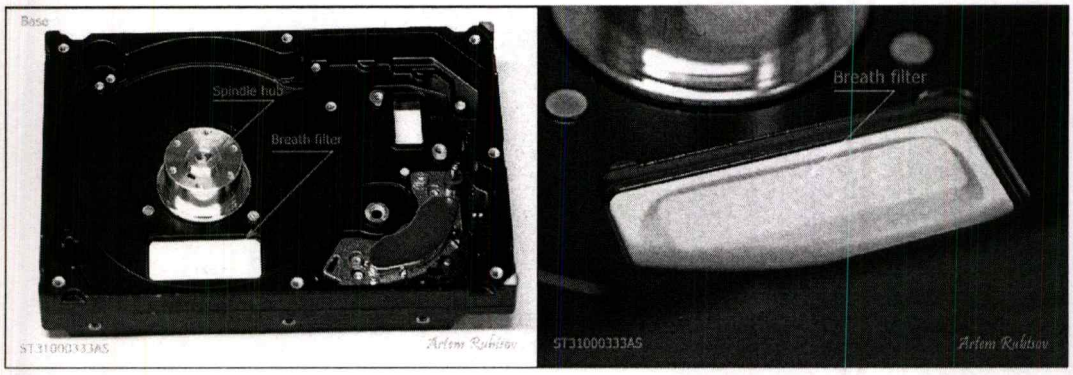

Figure 2.5 Hard disk drive (HDD)

http://hddscan.com/doc/HDD_from_inside.html

The distance from the platters to the heads is a specific design parameter that is tightly controlled by the engineers that create the drive. By adjusting the strength of the springs to match with the other drive parameters (such as the speed the disks are spinning and the size and shape of the heads) the float height can be precisely maintained. If the height is too great, the heads can't properly read and write the platter. If it is too small, there is increased chance of a head crash. As mentioned in the introduction, increasing areal density means that weaker magnetic fields must be used in storing data on the disks. When this is done the heads must be allowed to ride closer and closer to the platter surface to pick up the weaker signals, which requires other quality improvements to the drive to make sure that there is no chance of a head crash. Some modern drives include sensors that monitor the flying height of the heads and signal a warning if the parameter falls out of the acceptable range.

It's actually quite amazing how close to the surface of the disks the heads fly without touching. To put it into perspective, a modern hard disk has a flying height less than 10 nanoinches. A human hair has a thickness of over 2,000 micro inches. That is why keeping dirt out of the hard disk is so important! In fact, the floating height of a hard disk is smaller than the circuit size of a microprocessor.

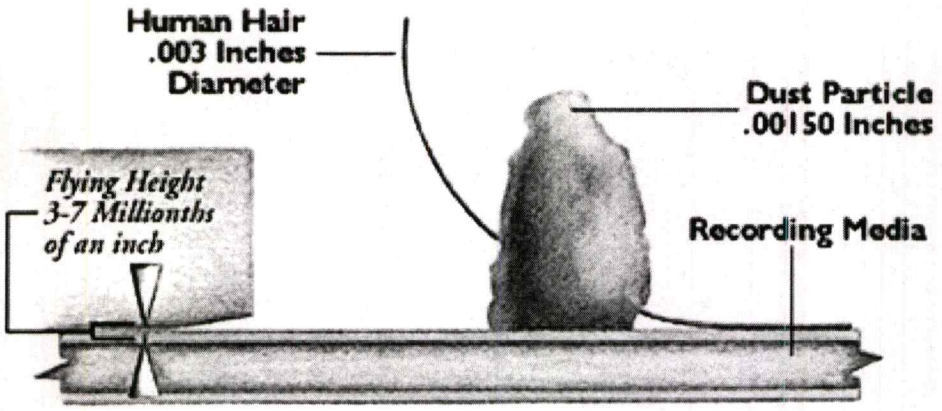

Figure 2.6 How small the flying height of a modern hard disk

When the areal density of a drive is increased to improve capacity and performance, the magnetic fields are made smaller and weaker. To compensate, either the heads must be made more sensitive, or the floating height must be decreased. Each time the floating height is decreased, the mechanical aspects of the disk must be adjusted to make sure that the platters are flatter, the alignment of the platter assembly and the read/write heads is perfect, and there is no dust or dirt on the surface of the platters. Vibration and shock also become more of a concern, and must be compensated for. This is one reason why manufacturers are turning to smaller platters, as well as the use of glass platter substrates. Newer heads such as TMR are preferred because they allow a higher flying height than older, less sensitive heads, all else being equal.

As the flying height of drives continues to decrease, hard disk engineers are recognizing that we may soon reach the point where it cannot be made any smaller without touching the surfaces of the platters. There is actually talked about the possibility of going back to the concept of contact disks, where the head gap is intentionally made zero. This would allow even smaller magnetic fields than is possible in today's drives. Of course, this brings us full circle to the first hard disk experiments in the 1950. The difference of course is almost 50 years of advances in technology. For example, thin film media is much tougher than the oxide media used on contact disks half a century ago and lubricating agents are much more advanced as well. Even so, it will probably be several years before we know if this technology will be feasible from both an engineering and manufacturing standpoint.

2.2 Lasers for interferometry

Several types of interferometers require a point source of monochromatic light. The closest approximation to such a source was, for many years, a pinhole illuminated by a mercury vapor lamp through a filter selecting a single spectral line. However, such a thermal source had two major drawbacks. One was the very small amount of light available; the other was the limited spatial and temporal coherence of the light. The laser has eliminated these problems and provides an intense source of light with a remarkably high degree of spatial and temporal coherence.

Some lasers that are commonly used for interferometry are listed in Table 2.1. Helium-neon (He-Ne) lasers are widely used for interferometry because they are inexpensive and provide a continuous, visible output. They normally operate at a wavelength of 633 nm, but modified versions are available with useful outputs at other visible and infrared wavelengths.

Table 2.1 Lasers for Interferometry [8]

Laser type	Wavelength (μm)	Output
He – Ne	3.39, 1.15, 0.63, 0.61, 0.54	0.5 – 25 mW
Ar^+	0.51, 0.49, 0.35	0.5 W – a few W
Diodee	1.064, 0.780, 0.660, 0.635, 0.594, 0.532, 0.475, 0.405	5 – 50 mW
Dye	1.08 – 0.41	10 – 100 mW
CO_2	9.4, 4.6	Few W – few kW
Ruby	0.69	0.6 – 10 J
Nd - YAG	1.06	0.14, 15 J

Argon-ion (Ar^+) lasers are more expensive but can provide much higher outputs. They can be operated at any one of a number of wavelengths in the visible and near UV regions, of which the strongest are those listed.

Laser diode systems now provide a range of wavelengths from the near infrared to the violet region of the spectrum. They are very compact and have low power consumption. A drawback with diode lasers is that the output beam is divergent and astigmatic. However, packages are available incorporating additional optics to produce a collimated beam. Diode lasers can be tuned over a limited wavelength range by varying the injection current.

Dye lasers can be tuned over a range of 50-80 nm with any given dye. Operation at any wavelength in the visible region is possible by choosing a suitable dye.

Carbon dioxide lasers can be operated at a number of wavelengths in two bands in the infrared region. Because of their long output wavelength, they are useful for measurements over long distances.

Very short pulses of light (< 20ns duration), with very high peak powers, are produced by ruby and Nd-YAG lasers.

Shorter wavelengths can be produced with diode and solid-state lasers by using a nonlinear crystal as a frequency doubler.

2.3 Photodiodes (Photo detectors)

Photodiodes use a junction between p- and n-type semiconductors to detect light. An n-type semiconductor contains many highly mobile electrons, while a p-type material contains less mobile positive holes. When two such materials are joined, the electrons and holes are drawn to opposite sides of the junction, and an energy level structure similar to that shown in Figure 7.2 is obtained. The region near the junction contains virtually no electrons or holes and is known as the depletion layer.

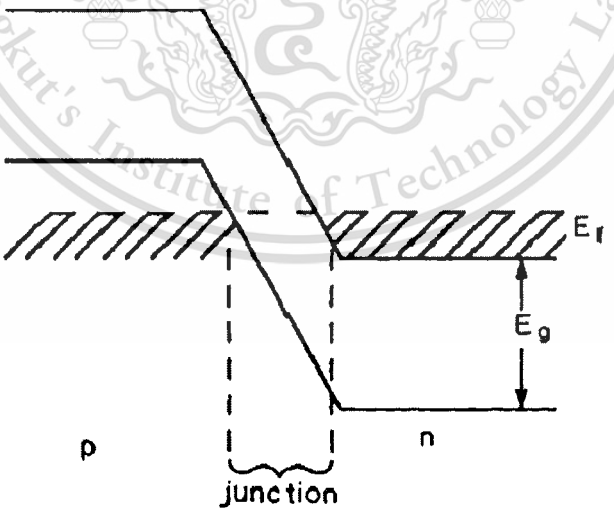

Figure 2.7 Energy level structure of a p-n junction [8]

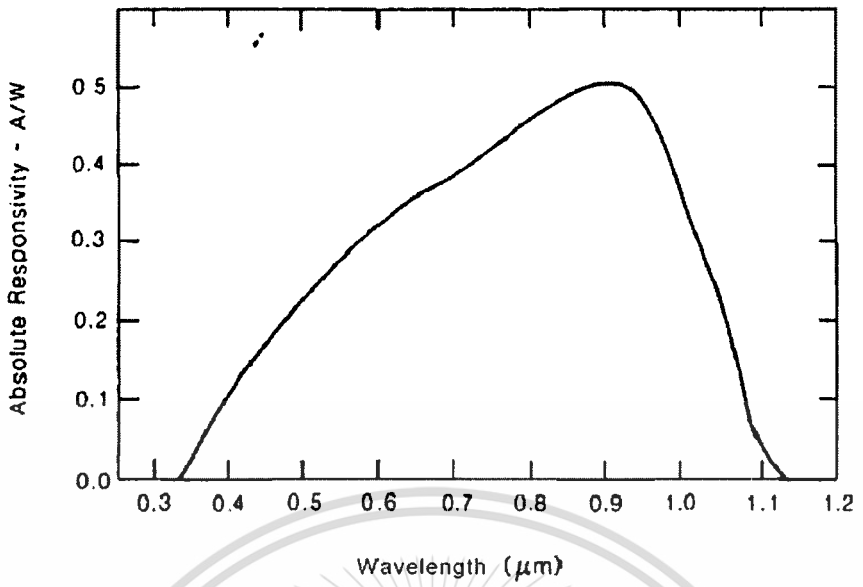

Figure 2.8 Typical spectral response of a silicon photodiode [8]

When the junction is illuminated, valence-band electrons are excited to the conduction band, creating electron-hole pairs. Because of the strong potential gradient in the junction region, the electrons and holes are accelerated in opposite directions, and a current flow.

The speed of response and sensitivity of a photodiode can be increased by reverse biasing; the positive side of a battery is connected to the n-type material and the negative side to the p-type material. Higher sensitivity can also be obtained by introducing a layer of a high-resistivity (intrinsic) material between the p- and n-layers; such a device is known as a p-i-n (or PLN) diode. PIN diodes have a useful response up to a frequency of a few hundred MHz.

With a sufficiently high reverse bias, electron multiplication due to secondary emission can occur. This effect is utilized in avalanche photodiodes to obtain a gain in sensitivity by a factor of a few hundred, but at the expense of an increase in noise at low light levels. Photodiodes are also available in a package that contains a high-gain operational amplifier. These devices can be used at very low light levels and, unlike photomultipliers, require only a low voltage. A linear relationship between output voltage (or current) and the light level can be obtained over several decades.

Silicon photodiodes are the most commonly used and, as shown in Figure 2.7, have peak sensitivity around 0.8-0.9 um. Germanium and InGaAs photodiodes are useful in the region from 1.1 to 1.7 um.

2.4 Basics of Interferometry

When an extended monochromatic source (such as a mercury vapor lamp with a monochromatic filter) is used, instead of a monochromatic point source, interference fringes are usually observed with good contrast only in a particular region. This phenomenon is known as localization of the fringes and is related to the lack of spatial coherence of the illumination.

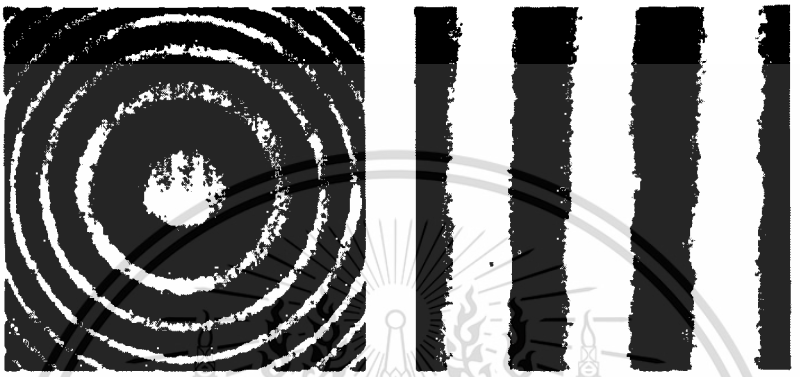

Figure 2.9 (a) Fringes of equal inclination, and (b) fringes of equal thickness [8]

For the present, it is enough to say that such an extended source can be considered as an array of independent point sources, each of which produces a separate interference pattern. If the optical path differences at the point of observation are not the same for waves originating from different points on the source, these elementary interference patterns will, in general, not coincide and, when they are superposed, will produce an interference pattern with reduced visibility. It can be shown that the region where the visibility of the fringes is a maximum (the region of localization of the interference fringes) corresponds to the locus of points of intersection of pairs of rays derived from a single ray leaving the source. Two cases are of particular interest. With a plane-parallel plate, aswe have seen earlier, any incident ray gives rise to two parallel rays that meet only at infinity. Accordingly, the interference fringes (fringes of equal inclination) formed with an extended quasi-monochromatic source is localized at infinity. If the fringes are viewed through a lens, as shown in Figure 2.2, they are localized in its focal plane.

In the case of a wedged thin film, as shown in Figure 2.3, a ray from a point source S gives rise to two reflected rays that meet at a point P. accordingly, with an extended source at S, the visibility of the interference pattern will be a maximum near P. In this case, the position of the region of localization of the interference fringe depends on the direction of illumination and can

shift from one side of the film to the other. However, for near-normal incidence, the interference fringes are localized in the film. To a first approximation, the interference fringes are then contours of equal thickness.

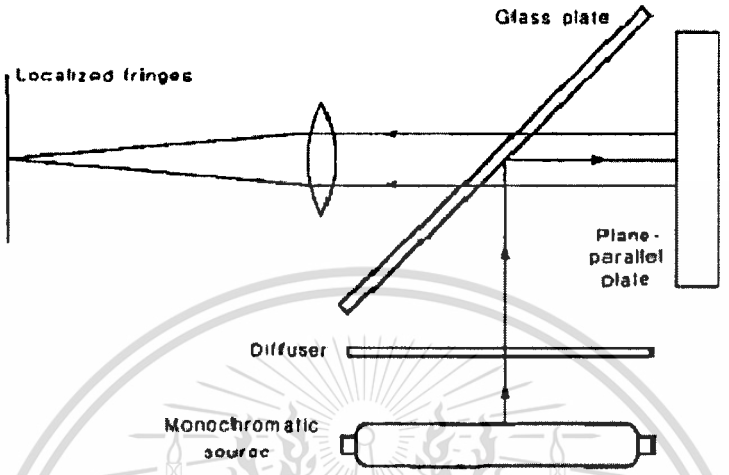

Figure 2.10 Interference with an extended light source, Formation of fringes of equal inclination localized at infinity [8]

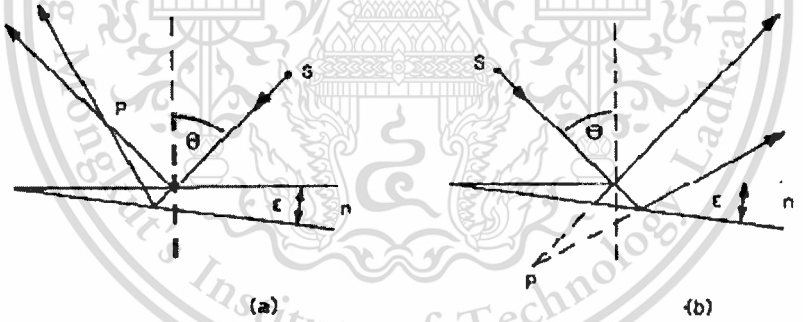

Figure 2.11 Formation with localized interference fringes by a thin wedged film [8]

2.5 Discrete Hilbert transform

To derive the discrete Hilbert transform we need the definition of the discrete Fourier transform (DFT) that is [7]

$$F[k]=\sum_{n=0}^{N-1} f[n]e^{-i\frac{2\pi}{N}kn}, \quad k=0,1,\ldots,N-1 \tag{1.1}$$

and the inversion formula [7]

$$f[n]=\frac{1}{N}\sum_{k=0}^{N-1} F[k]e^{i\frac{2\pi}{N}kn}, \quad n=0,1,\ldots,N-1 \tag{1.2}$$

where k is the discrete frequency and n is the discrete time. It is easy to prove (1.2) by inserting (1.2) into (1.1). Note that (1.2) defines aperiodic function with period N. Let us expand (1.1) in its real and imaginary parts on both sides, thus

$$F[k]=F_{Re}[k]+iF_{Im}[k],$$

and

$$\sum_{n=0}^{N-1} f[n]e^{-i\frac{2\pi}{N}kn}=\sum_{n=0}^{N-1} f[n]\cos\left(\frac{2\pi}{N}kn\right)-i\sum_{n=0}^{N-1} f[n]\sin\left(\frac{2\pi}{N}kn\right)$$

The real and imaginary part is now identified as

$$F_{Re}[k]=\sum_{n=0}^{N-1} f[n]\cos\left(\frac{2\pi}{N}kn\right),$$

$$F_{Im}[k]=-\sum_{n=0}^{N-1} f[n]\sin\left(\frac{2\pi}{N}kn\right),$$

and we conclude that $F_{Im}=0$ when k = 0 and k = N/2 . As we have seen before the Hilbert transform of the delta pulse $\delta(t)$ give us the Hilbert transformer $1/(\pi t)$ and the Fourier transform of the Hilbert transformer gives us the sign shift function $-i\,\mathrm{sgn}(\omega)$, that is [7]

$$\delta(t)\overset{H}{\Leftrightarrow}\frac{1}{\pi t}\overset{F}{\Leftrightarrow}-i\,\mathrm{sgn}(\omega) \tag{1.3}$$

The discrete analogue of the Hilbert transformer in (1.3) for even N is therefore given by

$$H[k]=\begin{cases} -i \text{ for } k=1, 2, \ldots, \dfrac{N}{2}-1 \\ 0 \text{ for } k=0 \text{ and } \dfrac{N}{2} \\ i \text{ for } k=\dfrac{N}{2}+1, \ldots, N-2, N-1 \end{cases}$$

and H[k] can be written on the form [7]

$$H[k]=-i\,\mathrm{sgn}\left(\frac{N}{2}-k\right)\mathrm{sgn}(k) \tag{1.4}$$

Here we have used the convention that $\mathrm{sgn}(0)=0$. The discrete frequency k is called positive in the interval $0<k<N/2$ and negative in the interval $N/2<k<N$ and alternate sign at $N/2$.

The discrete inverse Fourier transform of the discrete Hilbert transformer in (1.4) gives us the discrete impulse response in the time domain, for even N, thus [7]

$$\begin{aligned} h[n] &= \frac{1}{N}\sum_{k=0}^{N-1} H[k]e^{i\frac{2\pi}{N}kn} \\ &= \frac{1}{N}\sum_{k=0}^{N-1} -i\,\mathrm{sgn}\left(\frac{N}{2}-k\right)\mathrm{sgn}(k)e^{i\frac{2\pi}{N}kn} \\ &= \frac{2}{N}\sum_{k=1}^{\frac{N}{2}-1}\sin\left(\frac{2\pi}{N}kn\right), \end{aligned} \tag{1.5}$$

and h[n] can be expressed in closed form as [7]

$$h[n]=\frac{2}{N}\sin^2\left(\frac{\pi n}{2}\right)\cot\left(\frac{\pi n}{N}\right) \tag{1.6}$$

The function is given by the cotangent function with ever second sample (n = 0, 2, 4, …) erased by $\sin^2\left(\frac{\pi n}{2}\right)$, see Figure 2.12

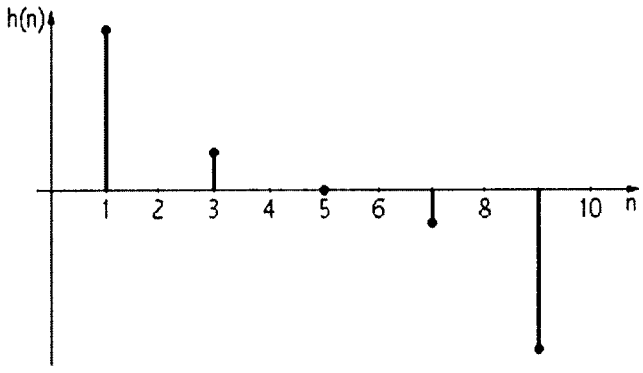

Figure 2.12 The discrete impulse response of the Hilbert transform for even N (N = 10) given by the cotangent function with ever second sample (n = 0, 2, 4, ...) erased by $\sin^2\left(\frac{\pi n}{2}\right)$ [7]

The same derivation for odd N is given by

$$H[k] = \begin{cases} -i \text{ for } k = 1, 2, \ldots, \frac{(N-1)}{2} \\ 0 \text{ for } k = 0 \\ i \text{ for } k = \frac{(N+1)}{2}, \ldots, N-2, N-1 \end{cases}$$

It is written on the same closed form as in the even case with the difference that there is no cancellation for $\frac{N}{2} - k$ that is [7]

$$H[k] = -i\,\mathrm{sgn}\left(\frac{N}{2} - k\right)\mathrm{sgn}(k) \tag{1.7}$$

The discrete impulse response for odd N of the Hilbert transformer in (1.3) is given by the discrete inverse Fourier transform of H[k] in (1.7), thus

$$h[n] = \frac{2}{N}\sum_{k=1}^{\frac{N-1}{2}} \sin\left(\frac{2\pi}{N} kn\right),$$

where the closed form of h[n] can be expressed as [7]

$$h[n] = \frac{1}{N}\left(\cot\left(\frac{\pi n}{N}\right) - \frac{\cos(\pi n)}{\sin\left(\frac{\pi n}{N}\right)}\right) \tag{1.8}$$

As we mentioned before we do not have the same cancellation for odd N as for even N (1.6), instead h[n] is changing sign by odd and even values of n, see Figure 2.13

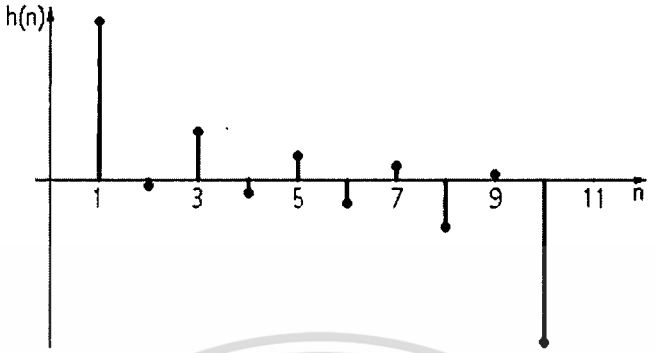

Figure 2.13 The discrete impulse response of the Hilbert transform for odd N (N = 11) with every second sample positive with next sample negative [7]

2.6 Literature review

Up to now, there are many methods based on optical interferometry have been developed to measure nano-scale spacing of head flying height. In this thesis, we have reviewed the 4 powerful methods. Intensity interferometry, polarization interferometer, phase comparison michelson interferometry and dual-beam normal incidence polarization interferometry.

2.6.1 Intensity Interferometry

Xinqun Liu *et,al.*[2] mentioned about a method that use to implement in the industry to determine the absolute flying height.

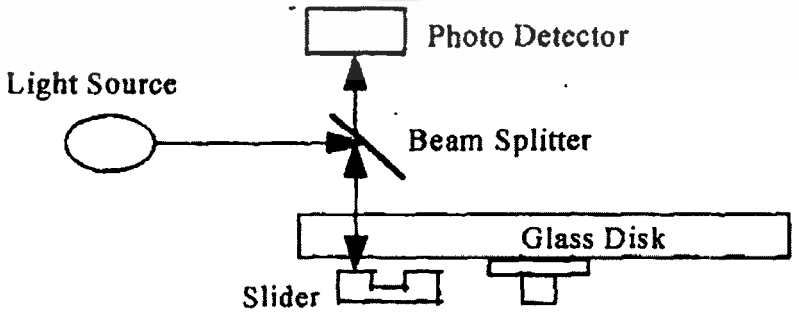

Figure 2.14 Schematic of a flying height tester base on intensity interferometry [2]

A schematic of a modern flying height tester based on intensity interferometer is shown in Fig. 1 in which a normal incidence beam is usually employed. At the slider-disk interface, the light beam actually experiences a multi-reflection. In such an instance, the intensity of the interfered light reflected from the slider-disk interface is given by the standard thin-film equation as below [2].

$$I = I_0 \frac{r_1^2 + |r_2|^2 + 2r_1|r_2|\cos(\delta + \phi_s)}{1 + r_1^2 + |r_2|^2 + 2r_1|r_2|\cos(\delta + \phi_s)}$$

Where $\delta = \frac{4\pi h}{\lambda}$, $\phi_s = \pi - \tan^{-1}\left(\frac{2n_0k_1}{n_0^2 - n_1^2 - k_1^2}\right)$,

$r_1 = \frac{n_2 - n_0}{n_2 + n_0}$, $r_2 = \frac{n_0 - (n_1 + ik_1)}{n_0 + (n_1 + ik_1)}$, h is the flying height,

λ is the light wavelength, n_0, $(n_1 + ik_1)$, n_2 are refractive

Indices of the air, slider and glass respectively

From the above equation the plot of the normalized intensity I/Io as a function of flying height h in Figure 2.8

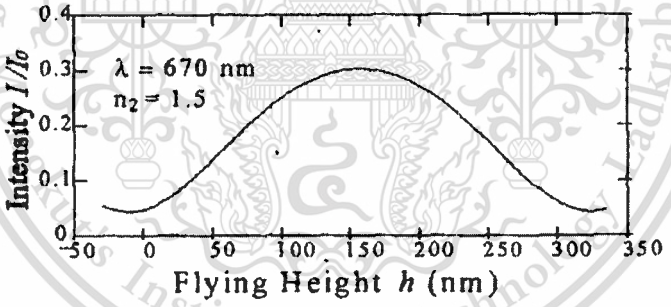

Figure 2.1 5Reflected intensity as a function of flying height [2]

It can be seen from the curves that the best sensitivity occurs around h = 60 nm, and calculations show that the sensitivity is reduced to half the maximum value at about h = 10 nm, and continues to worsen below this height even in the presence of, phase change on reflection phenomenon (PCOR).

2.6.2 Polarization Interferometer

The other method has studied by P. de Groot *et al* [1]. using polarization interferometer.In this method, about 50° oblique incidence is adopted to make the best use of the phase information. Theoblique incident laser beam defines two orthogonalpolarization

components s and p, where p polarization isparallel to the plane of incidence. The combined reflectionsfrom the slider-disk interface modify the polarization state ofthe beam. The intensity of the interfered light I and the phasedifference□between the two polarization components havethe following relationship with the flying height h. [2]

$$I(h) = I_{p0}|r_p(\beta)|^2 + I_{s0}|r_s(\beta)|^2$$

$$(h) = arg[r_s(\beta)] - arg[r_p(\beta)]$$

Where $\beta = 4\pi h \cos(\emptyset)/\lambda$, $I_{p0} = I_{s0} = I_0$, λ is thewavelength of the laser beam, $\emptyset$ is the incident angle, $I_{p0}$and $I_{s0}$are the intensities of the incident p polarized and spolarized light to the slider-disk interface, and r_p and r_s arethe effective reflectivity of the slider-disk combination.The intensity and phase curve is that theyare complementaryas shown in figure 2.17. When the intensity curve has a steepslope, the phase is fairly constant, when the intensity isnearly constant, the phase is changing rapidly. Using bothcurves together means that there always exists a way tomeasure flying height with positive sensitivity.

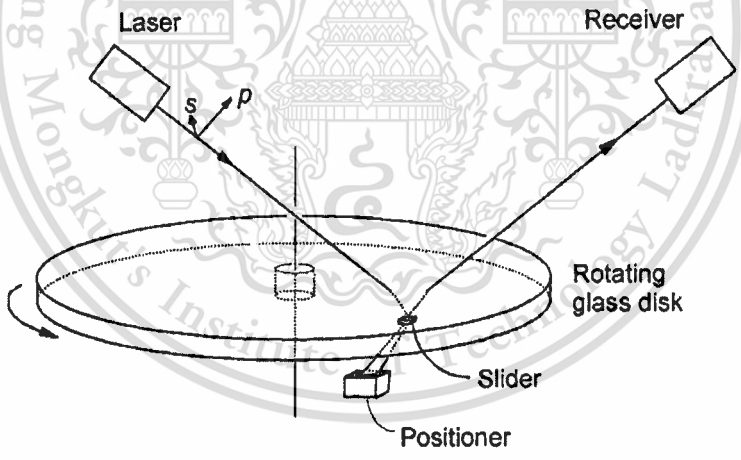

Figure 2.16 Polarization interferometer for flying-height testing of head sliders. [1]

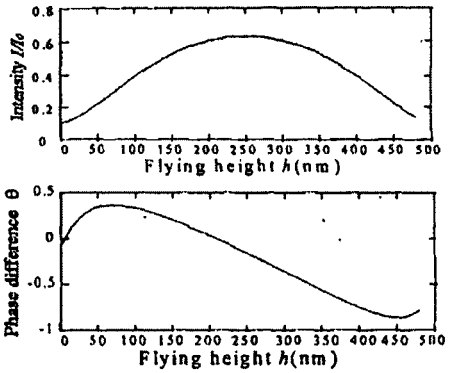

Figure 2.17 Intensity curve and phase difference curve [2]

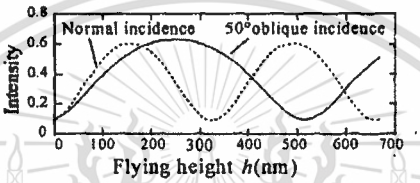

Figure 2.18 Intensity curves with different beam incidence conditions [2]

In summary and conclusions, they research shows that it is possible and practical to measure the optical constants of every slider during optical flying-height testing. But the disadvantage of this method is the sensitivity of the intensity channel is reducing by factor of 1/cosØ compare with that of the normal incidence as shown in figure 2.18.In addition to the disadvantages mentioned, because theyonly perform one point measurement at one time, neither ofthe above methods can perform dynamic measurement.

2.6.3 Phase Comparison Michelson Interferometry

The method that proposed by Yinbo He*et al.* call Fly Height Measurement Based on Phase Comparison Michelson Interferometry Using Low-Coherence Light Source [6]. They has developed by using phase comparison Michelson interferometry (PCMI), which compares the phases of two interference fringe patterns formed respectively on the inner surface of a glass disk and the air-bearing surface of a fly head slider through the glass disk. To suppress interference noise and further enhance measurement accuracy, they were used a low-coherence light source as an illumination source to replace a high-coherence laser. The captured fringe images enabled us to extract ridge lines much more accurately than with a laser. We compared our measurements in the sub-10 nm spacing range with calculations and found excellent agreement.

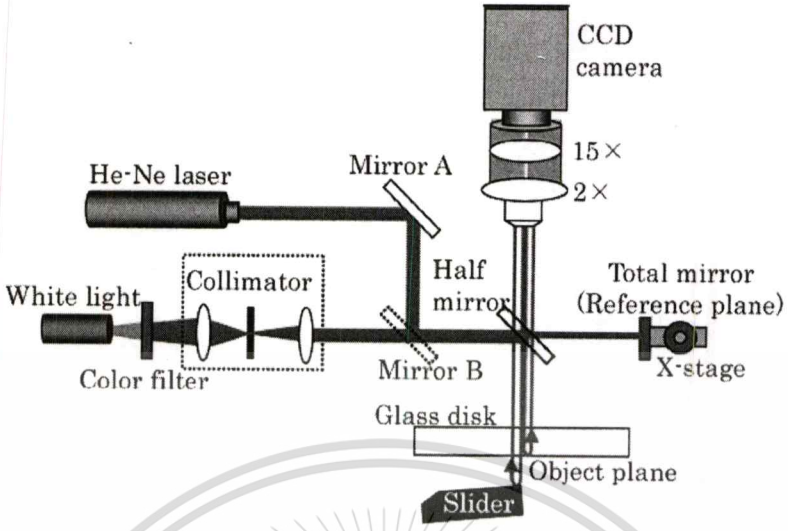

Figure 2.19 Optical system of the PCMI for fly height measurement [6]

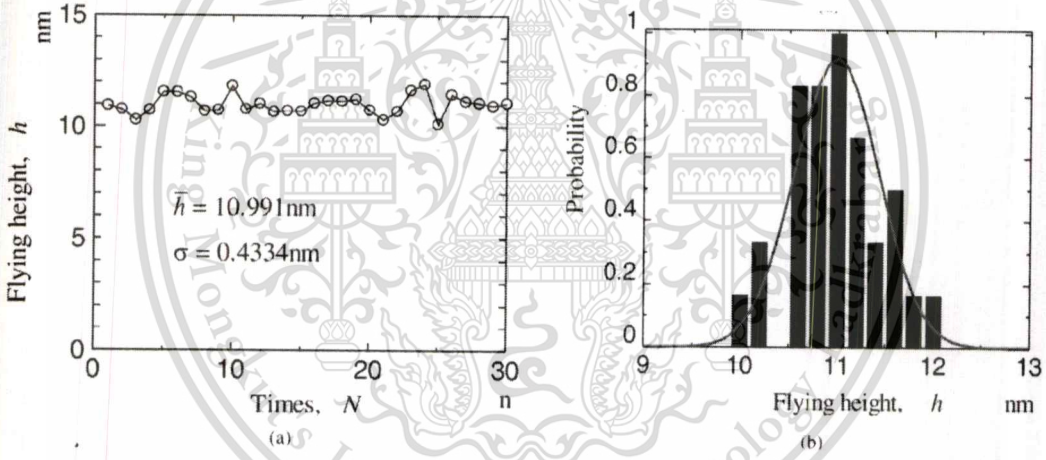

Figure 2.20 (a) Reproducibility of FH measurements. (b) Histogram of deviation. [6]

2.6.4 Dual-Beam Normal Incidence Polarization Interferometry

Base on the disadvantage of above methods Xinqun Liu *et al.* has proposed a dual-beam normal incidence polarization interferometry method [2] which is shown in Figure2.21.

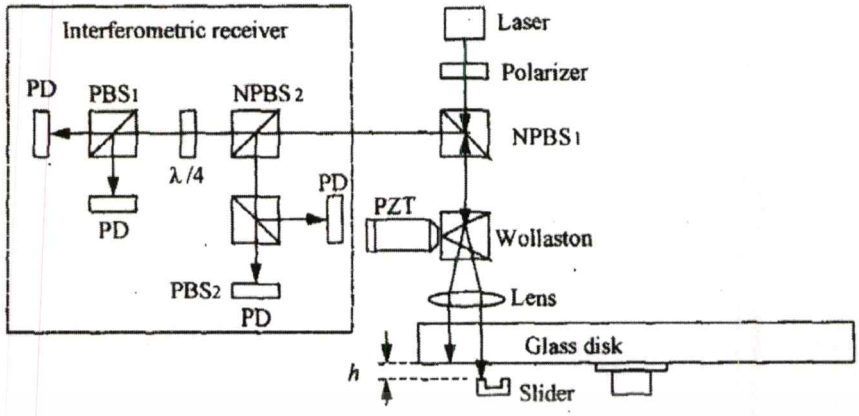

Figure 2.21 Dual-beam normal incidence polarization interferometry [2]

A 670 nm laser diode is used as the light source. The laser beam passes through a polarizer and a beam splitter. The exiting beam then passes through a Wollaston prism which splits the light into two orthogonally-polarized beams. The lens focuses these two beams on two close but distinct points on the slider air bearing surface and the glass disk. The reflected beams then pass through the Wollaston prism again and recombine to a single beam. This returning beam finallyenters the interferometric receiver which is used to measure the intensity and phase difference between the two polarization components of the returned beam. The interferometric receiver consists of a non-polarizing beam splitter, a quarter-wave plate, two polarizing beam splitters, and four photo detectors. The PZT translator is used to move the Wollaston prism so as to adjust the phase difference between the two polarization components.

The flying height is calculated by below phase differenceequation. And the phase difference between the head slider and media glass disk detected by the photo detectors.

$$\theta = \arg(r_{s20}) - \arg\left(\frac{r_{p20} + r_{p01}\exp(i\beta_p)}{1 + r_{p20}r_{p01}\exp(i\beta_p)}\right)$$

where $r_{p20} = \dfrac{n_2 - n_0}{n_2 + n_0}$, $r_{p01} = \dfrac{n_0 - (n_1 + ik_1)}{n_0 + (n_1 + ik_1)}$,

$\beta_p = \dfrac{4\pi}{\lambda} n_0 h$, λ is the wavelength, h is the flying height

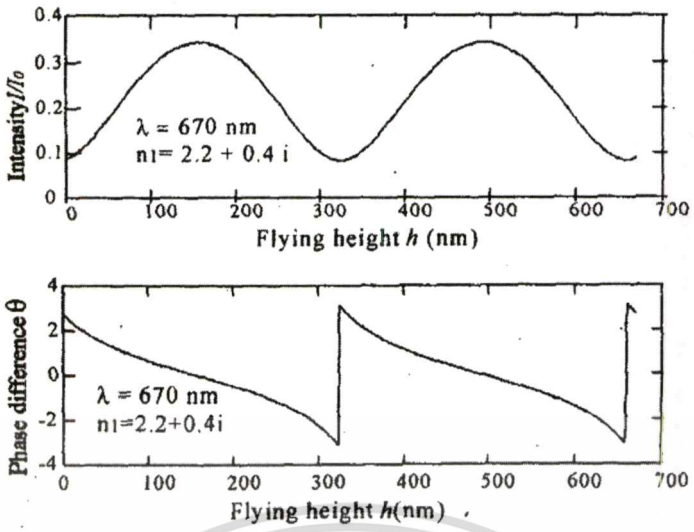

Figure 2.22 Intensity and phase difference as functions of flying height [2]

Theoretical analysis and numerical results show that the proposed method can be used for the flying height measurement down to contact. With greatly improved accuracy at small head-disk spacing compared to the existing intensity method, and with improved intensity channel sensitivity compared with the existing polarization interferometry method. It also shares the additional advantage with the oblique incidence polarization interferometer that the complex reflective index of the slider can be determined in-situ during the flying height testing which is an indispensable step for flying height measurement.

Chapter 3

Experiment and Result

In this study of the phase difference measurement using a one-dimensional discrete Hilbert transform for application in the recording head flying height tester, these evaluates are separated for 2 parts; firstly, fly height measurement at initial state which measure only the surface of media glass disk (without object plane) and then install the object plan for measurement the fly height at experiment state (measurement on Triangular wave spacing and measurement on Sine wave spacing.

Objective of this chapter is to validate the proposed flying height measurement set which developed base on Dual-beam normal incidence polarization interferometry. The optical interferometry is used for capturing interference signal instead of interferometry receiver. The interference signal is captured and calculated by using a one-dimensional discrete Hilbert transform. Advantage of the proposed method is to simplify the flying height measurement set with maintain sensitivity of the system.

3.1 Research tools and materials

To support the recording head flying height measurement using phase comparison Michelson interferometry, there are many parts were setup to constitute a dual beam optical system. First is a Helium Neon laser with an emitting wavelength 632.8 nm at maximum 0.5 mW which is used as a main laser source. A polarizer (Linear Polarizer, VIS 550 – 1500 nm) orients at 45° is used to separate the laser light into two polarization states. A non-polarizing beam splitter is split the beam to a reference and a sample beam. A beam displacing which is used to splits the sample beam to be the parallel beam. An experiment disk 3.5 inch diameter quartz disk with the 3 mm thickness and the top surface is coated with anti-reflective material. The mirrors are used for reference mirror and object plane. A piezoelectric actuator, max displacement 4.6 μm, 3.5 x 4.5 x 5 mm is used for varying the Fly height. A non-polarizing beam splitter is used for combining a reflect beam from the reference and the sample. The High-speed optical detectors are used for detecting the interference signals. A pulse generator is used for supply the pulse signal to a piezoelectric actuator for varying the Fly height. And a digital oscilloscope is used for capturing the interference signal from the High-speed optical detectors.

3.2 Fly Height Measurement at Initial state

3.2.1 Experiment setup

The Fly height measurement based on phase difference measurement using a one-dimensional discrete Hilbert transform is shown in figure 3.1 A Helium Neon laser with an emitting wavelength 632.8 nm at maximum 0.5 mW is used as a laser source. The laser beam passes through a linear polarizer which separates the laser light into two polarization states and a non-polarizing beam splitter (NPBS). The sample beam then passes through a beam displacing which splits the parallel beam into an experiment disk (3.5 inch diameter quartz disk with the 3 mm thickness and the top surface is coated with anti-reflective material). The two beams are reflected at the no coat surface of an experiment disk and travel back through a beam displacing again and combining to the single beam then passes through a non-polarizing beam splitter. At the non-polarizing beam splitter, all beams are combining and interface with each other. The polarizing beam splitter (PBS) is split all beam into two orthogonal polarization states which represent to each component, and detect the interference signal by the high-speed optical detectors.

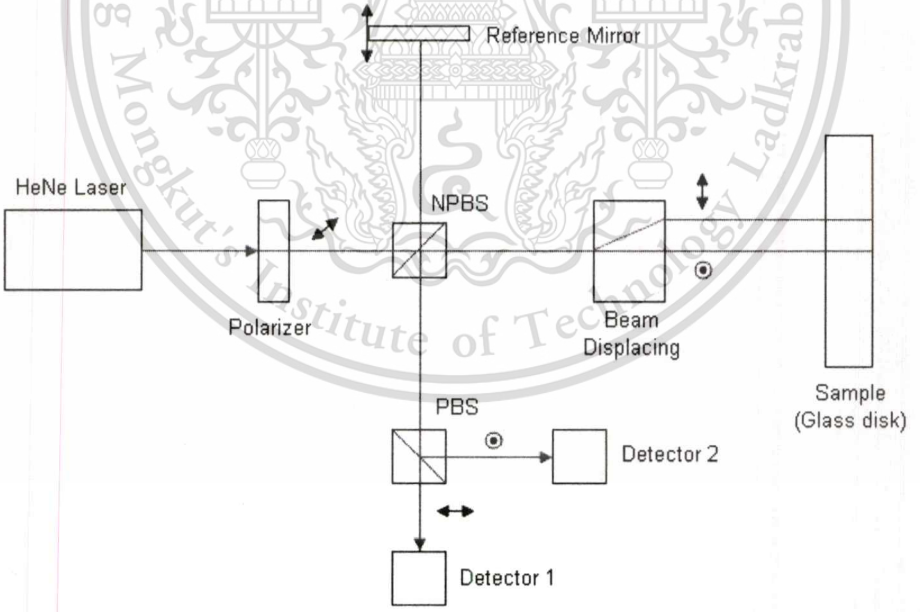

Figure 3.1 Optical system of phase difference measurement in flying height tester for initial state

3.2.2 Methodology

The objectives for calculate phase difference and fly height at the initial state (without object plane) by measuring fly height only at the surface of media glass disk. The two measurement beams which reflecting at the 2 no coat surfaces of an experiment media glass disk are capture by high-speed optical detectors. Then use digital oscilloscope measuring the interference the signal from both detectors and record the result in text file format. The calculation is using Matlab program for calculate the phase difference. The data collecting is shown in figure 3.2

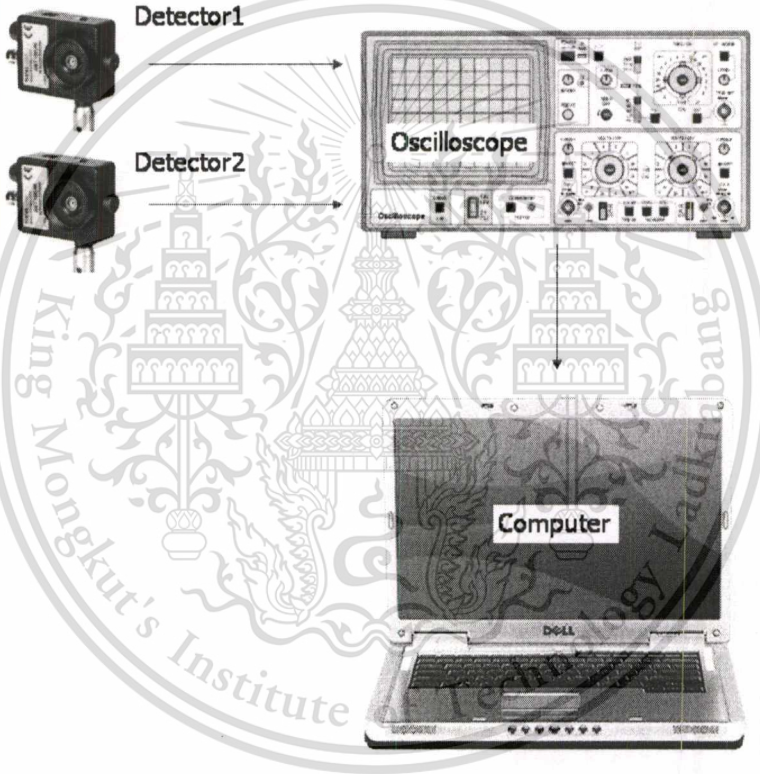

Figure 3.2 Data collecting and data computation of the fly height measurement

3.2.3 Data Computation

The objectives of this evaluation to calculate the phase difference then fly height at the initial state (without object plane). The methodology is to use digital oscilloscope to measure the interference signal which captured from both detectors then calculate the fly height per below procedure.

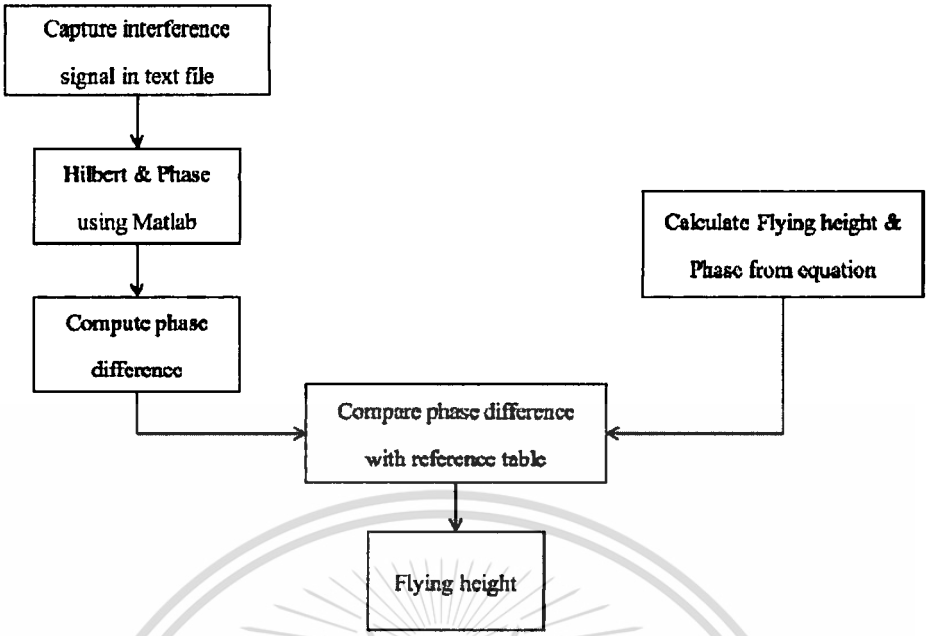

Figure 3.3 Data computation flow

1. Calculate the reference fly height base on the phase difference (radian) for calculating the actual flying height from the experiment follow figure 3.1. By using the standard thin-film equation (3.1)

$$\theta = \arg(r_{s20}) - \arg\left(\frac{r_{p20} + r_{p01}\exp(i\beta_p)}{1 + r_{p20}r_{p01}\exp(i\beta_p)}\right) \qquad (3.1)$$

By θ is phase difference between the two polarization components

$$r_{s20} = \frac{n_2 - n_0}{n_2 + n_0}$$

$$r_{p20} = \frac{n_2 - n_0}{n_2 + n_0}$$

$$r_{p01} = \frac{n_0 - (n_1 + ik_1)}{n_0 + (n_1 + ik_1)}$$

$$\beta_p = \frac{4\pi}{\lambda} n_0 h$$

λ is the wavelength

h is the fly height

n_0, $n_2$and (n_1+ik_1) are the refractive indices of glass, air, and slider material respectively

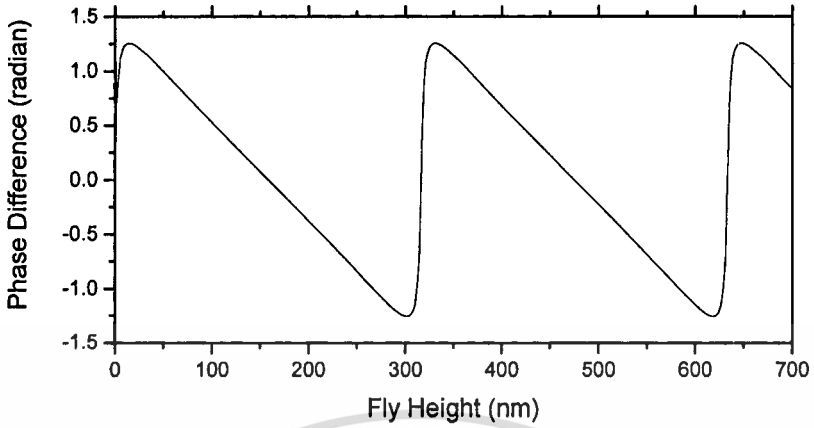

Figure 3.4 Phase difference as function of fly height for reference

2. From the result of an evaluate follow figure 3.1, the 2 interference signals is capture (detector 1 & 2) in text file that shown as figure 3.2.

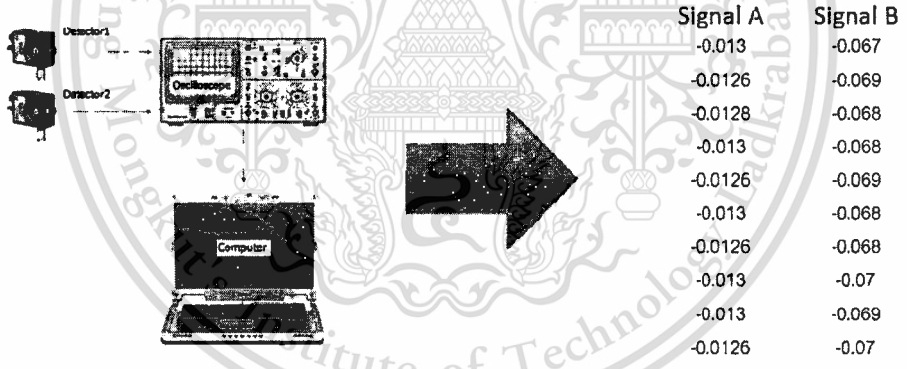

Figure 3.5 The 2 interference signals captured by oscilloscope

3. Use Hilbert transform to calculate the interference signal.
    a. 3.1 Hilbert uses a four-step algorithm:
        i. It calculates the FFT of the input sequence, storing the result in a vector F[k].
        ii. It creates a vector h whose elements h(k) have the values:
            1. 1 for i = 1, (n/2)+1
            2. 2 for i = 2, 3, ... , (n/2)
            3. 0 for i = (n/2)+2, ... , n

iii. It calculates the element-wise product of F[k] and h(k).

iv. It calculates the inverse FFT of the sequence obtained in step 3 and returns the first n elements of the result.

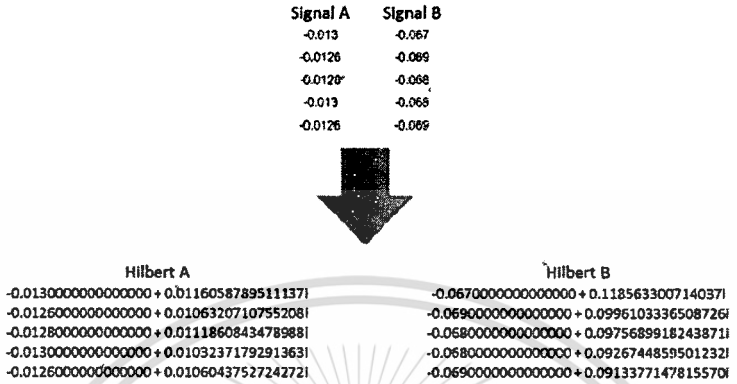

Figure 3.6 Hilbert calculation result

4. Calculate phase referring to Trigonometric function that shown as equation (3.2)

$$\square = \text{atan}\frac{X(imaginary)}{X(real)} \quad (3.2)$$

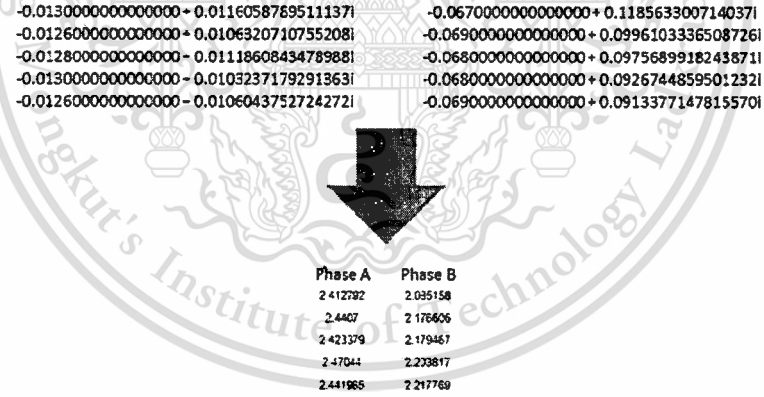

Figure 3.7 Phase calculation result

5. Calculate the phase difference by compare both phase together (Phase A – Phase B).

Phase A	Phase B	Phase difference (Θ)
2.412792	2.085158	-0.327634135
2.4407	2.176606	-0.26409457
2.423379	2.179467	-0.243911236
2.47044	2.203817	-0.26662319
2.441985	2.217769	-0.224216664
2.471331	2.23329	-0.238040393
2.458997	2.227595	-0.231402475
2.467938	2.259778	-0.208160503
2.495755	2.261673	-0.234082631
2.480432	2.279725	-0.200707672

Figure 3.8 Phase difference comparison result

6. Calculate the actual flying height by interpolate the phase difference result with the reference flying height as figure 3.4

Phase difference (Θ)	Flyheight
-0.33	195
-0.26	187
-0.24	185
-0.27	188
-0.22	183
-0.24	185
-0.23	184
-0.21	182
-0.23	184
-0.2	181

Phase Difference	Flyheight
0.96	54
0.95	55
0.94	56
0.93	57
0.92	58
0.91	59
0.90	60
0.89	61
0.88	62
0.87	63

Figure 3.9 Flying height calculation result by interpolate the phase difference result with the reference flying height

3.2.4 Experiment Result and Discussion

The interference signals that reflected from experiment glass disk and combining with reference beam as shown in figure 3.10, solid and dash curves represent the interference signal from detector1 and detector2 respectively.

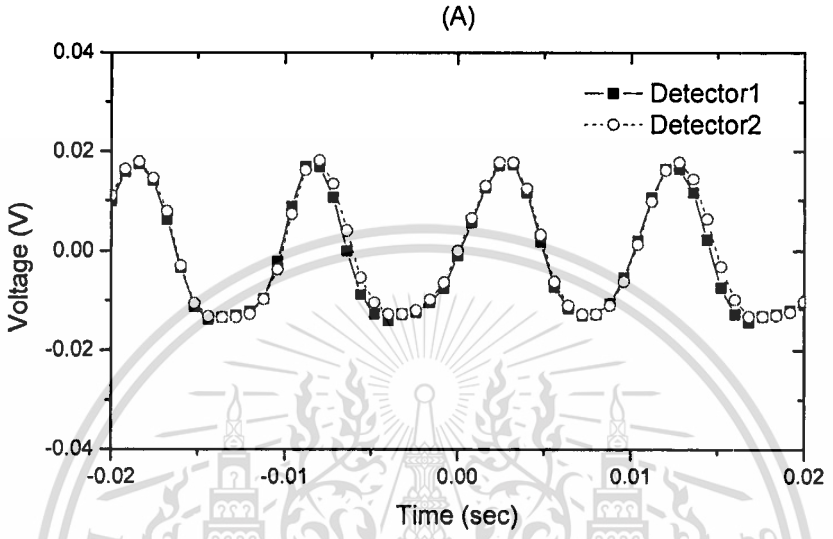

Figure 3.10 Interference signal of the experiment glass disk

Figure 3.11 shows the calculation of One-dimensional discrete Hilbert transform and phase distribution (in radians), the result show -0.08 radians phase difference and compute to distance at 8.02 nanometers which is very close to zero as shown in figure 3.12.

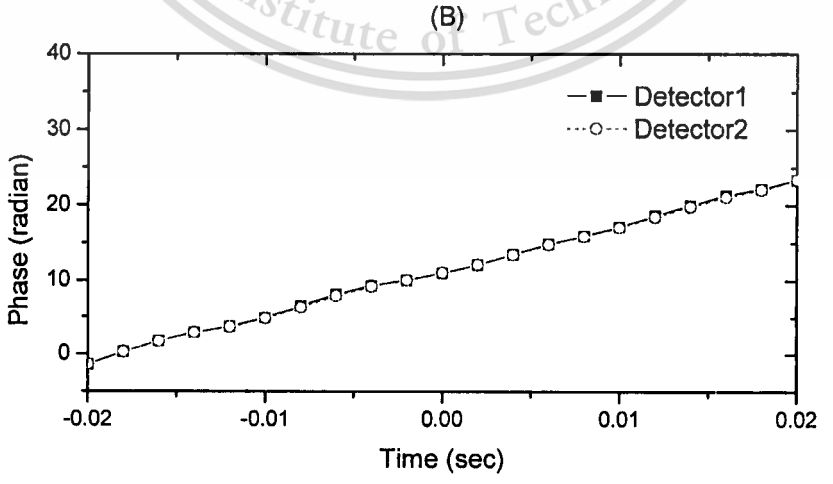

Figure 3.11 Phase calculation of the Hilbert transform (without object plane)

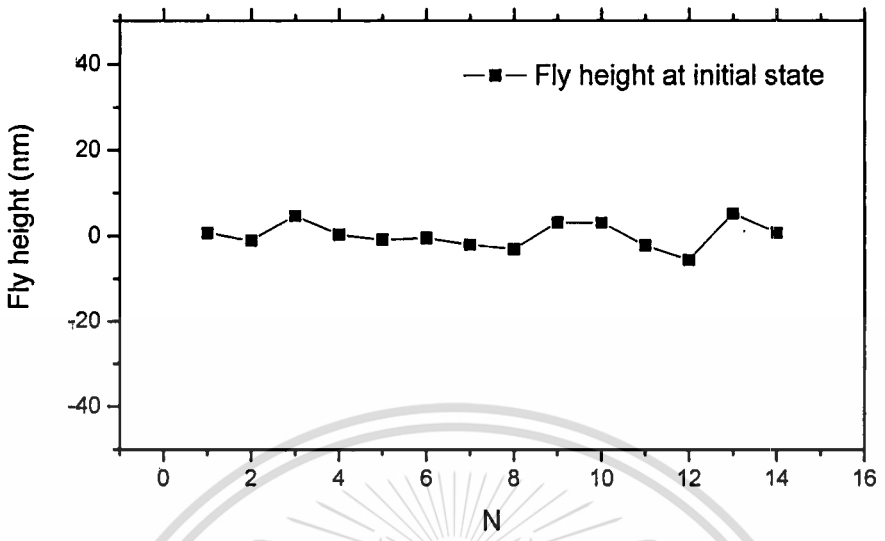

Figure 3.12 Calculation result of experiment glass disk (without object plane)

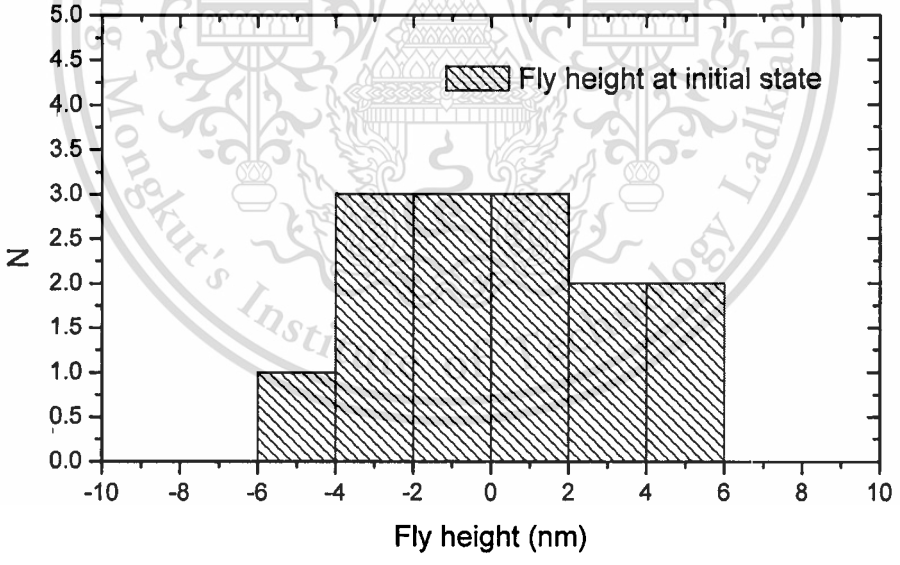

Figure 3.13 Histogram of deviation (STDEV = 3)

To evaluate the reproducibility of the system, flying height at ainitial state were measured 14 times and summarized in Figure 3.13, X axis is flying height (nm) and Y axis is quantity (N). The corresponding normalized histogram tends to follow well a Gaussian

distribution and standard deviation is 3 nm. The random variations of flying height are come from contamination and various vibrations from system and environment.

3.3 Fly Height Measurement at experiment state (with Object plane)

Objective of this evaluate for measurement and calculate a flying height of the experiment glass disk and objective plane (experiment slider). An evaluation separated into 2 parts follow by the input signals which are Triangular wave pulse and Sine Wave pulse.

3.3.1 Experiment Setup

The schematic of phase difference measurement in flying height tester for measurement state shown in Figure 3.14, the evaluation has install the object plane (experiment slider) which are the experiment slider and piezoelectric actuator that use for adjust the distance between experiment slider and experiment glass disk in nano-scale. From figure 3.14, NPBS is non-polarizing beam splitter, PBS is polarizing beam splitter and PZT is piezoelectric actuator.

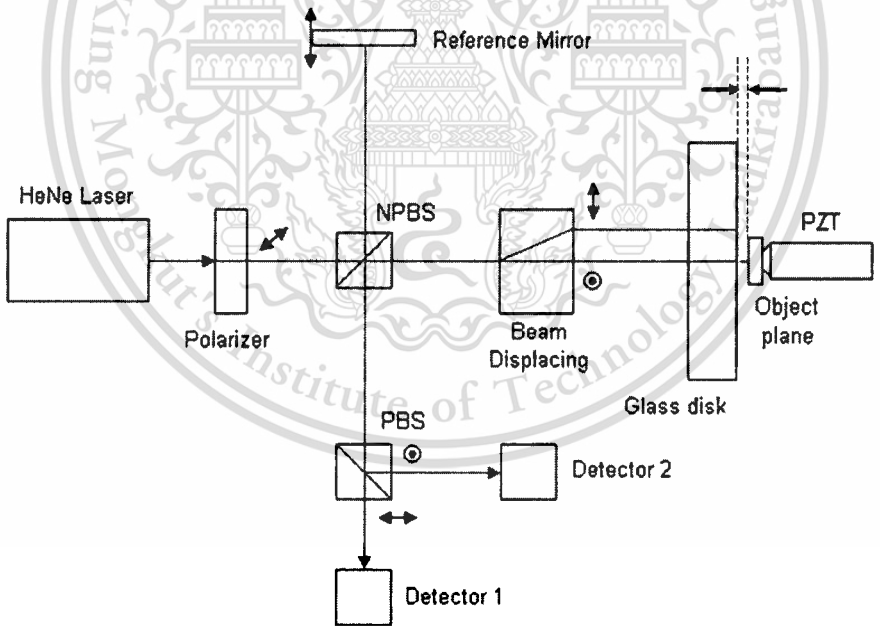

Figure 3.14 Optical system of phase difference measurement in flying height tester for measurement state

3.3.2 Flying height measurement with Triangular wave signal

This evaluation will apply the Triangular wave pulse to Piezoelectric actuator for vary the distance between experiment glass disk and slider. The interference signal is captured form both detectors use for calculate the actual flying height as same as the evaluation item 3.2

1. Methodology

The Piezoelectric actuator use for adjust the distance of slider follow by the input signal. In this evaluate, we apply the Triangular wave pulse as shown in Table 3.1 that fix the frequency at 50 Hz and vary the amplitude from 5 to 20 volts. The piezoelectric actuator will move the slider in/out from glass disk as Triangular wave shape. Then use Oscilloscope to capture the interference signal from detector1 and detector2 for calculate the actual flying height as same as the method in evaluation item 3.2. The result of the evaluation will consider the actual flying height and shape of the flying height compare to the input signal

Table 3.1 Frequency and amplitude for evaluation

# Rec	Frequency (Hz)	Amplitude (V)
1	50	5
2	50	10
3	50	15
4	50	20

2. Experiment result of Flying height measurement with Triangular wave signal @ 50Hz

The interference signals that reflected from experiment glass disk and combining with reference beam as shown in figure 3.15, solid and dash curves represent the interference signal from detector1 and detector2 respectively. The phase difference as function of period (T) can be drawn as figure 3.16. Calculation is done by using Hilbert transform and Trigonometric function.

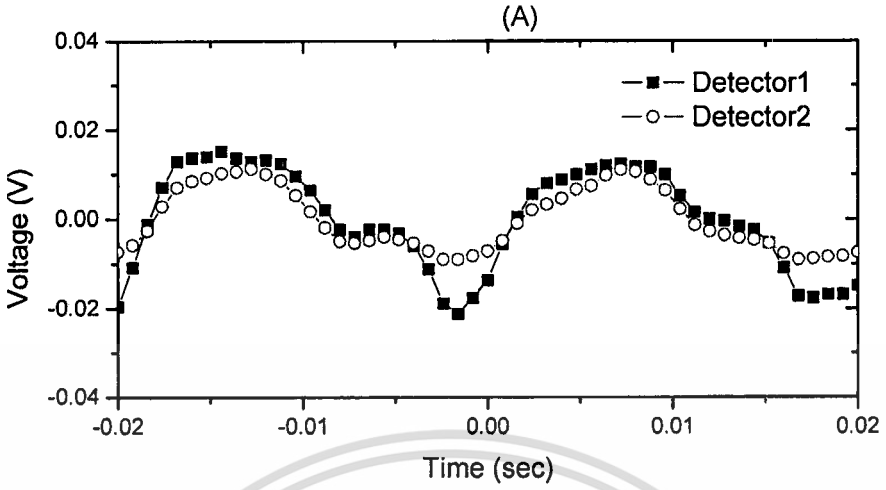

Figure 3.15 Interference signal of the experiment glass disk and object plane

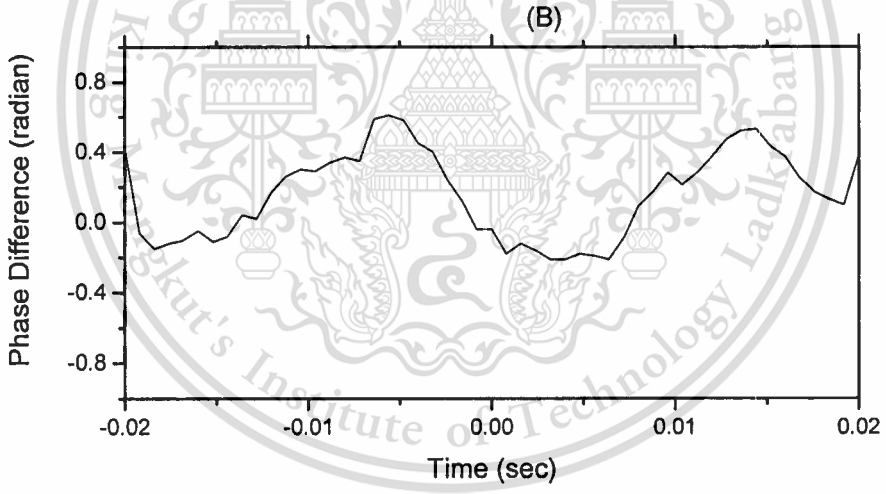

Figure 3.16 Phase calculation of the Hilbert transform for the one-dimensional phase distribution

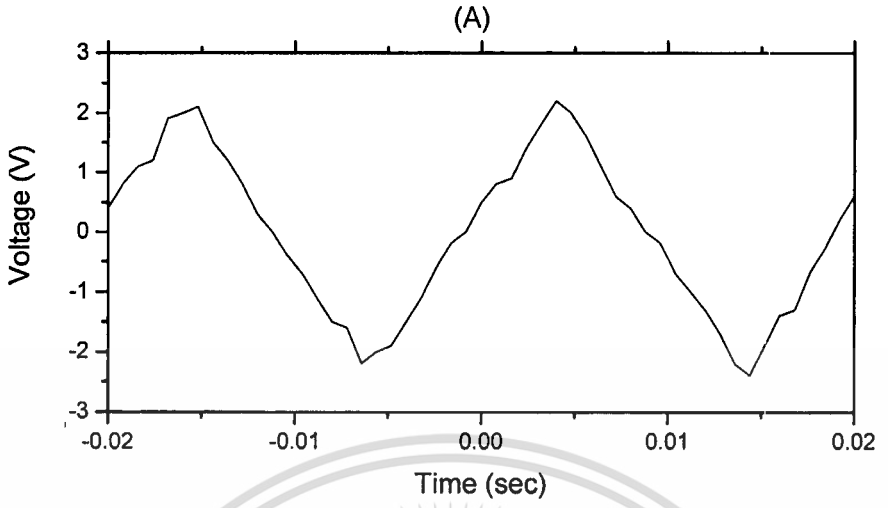

Figure 3.17 Input signal of piezoelectric actuator (@ 50Hz Triangular wave)

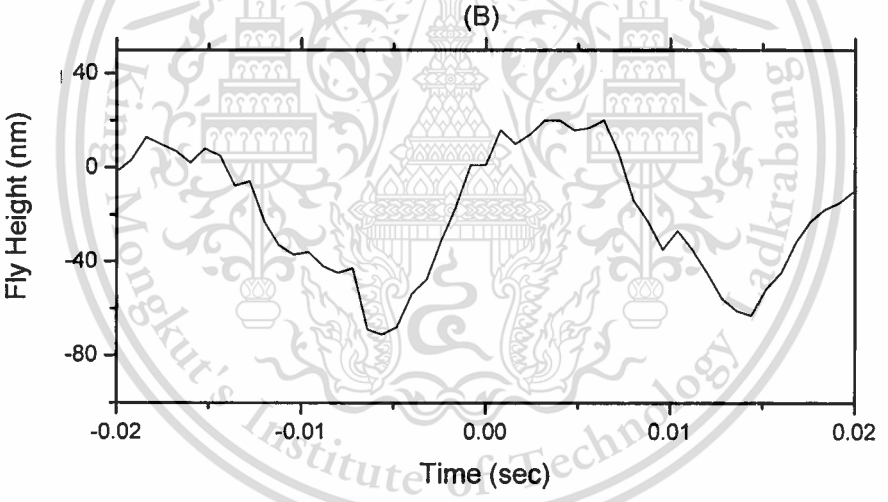

Figure 3.18 Fly height calculation result base on phase difference measurement method

From Figure 3.17 and 3.18, the input voltage (V) and flying height as function ofperiod (T), the vertical axis of the graph shows the calculated flying height and the horizontal axis of the graph shows the period (T). Result indicated that inputsignals sent to piezoelectric actuator (PZT) is similar shape with calculated flying height. By the way, variation on calculated flying height curve might come from responsibility and sensitivity of the piezoelectric actuator.

Table 3.2 Actual fly height and phase delay @ 50Hz Triangular wave

Rec#	Input Frequency (Hz)	Input Amplitude (V)	Fly height (P-P) (nm)	Phase Delay (mSec)
1	50	5	105	20
2	50	10	230	16
3	50	15	88	16
4	50	20	200	15

3.3.3 Flying height measurement with Sine wave signal

Refer to an evaluation item 3.3.2 the result showed that the shape of actual flying height is comparable to the input signal which supply to Piezoelectric actuator (PZT), the shape as same as Triangular wave pulse. For validate the system of phase measurement, this evaluation will apply the Sine wave pulse to Piezoelectric actuator for vary the distance between experiment glass disk and slider. The interference signal is captured form both detectors use for calculate the actual flying height as same as the evaluation item 3.2

1. Methodology

This evaluate will supply the Sine wave pulse to the Piezoelectric actuator for adjust the distance of slider follow by the input signal (50 Hz, 5 volts). The piezoelectric actuator will move the slider in/out from glass disk as sine wave shape. Then use Oscilloscope to capture the interference signal from detector1 and detector2 for calculate the actual flying height as same as the method in evaluation item 3.2. The result of the evaluation will consider the actual flying height and shape of the flying height compare to the input signal

Table 3.3 Frequency and amplitude for evaluation

# Rec	Frequency (Hz)	Amplitude (V)
1	50	5

2. Experiment result of Flying height measurement with Sine wave signal @ 50 Hz

The interference signals that reflected from experiment glass disk and combining with reference beam as shown in figure 3.19, solid and dash curves represent the interference signal from detector1 and detector2 respectively. The phase difference as function of period (T) can be drawn as figure 3.20. Calculation is done by using Hilbert transform and Trigonometric function.

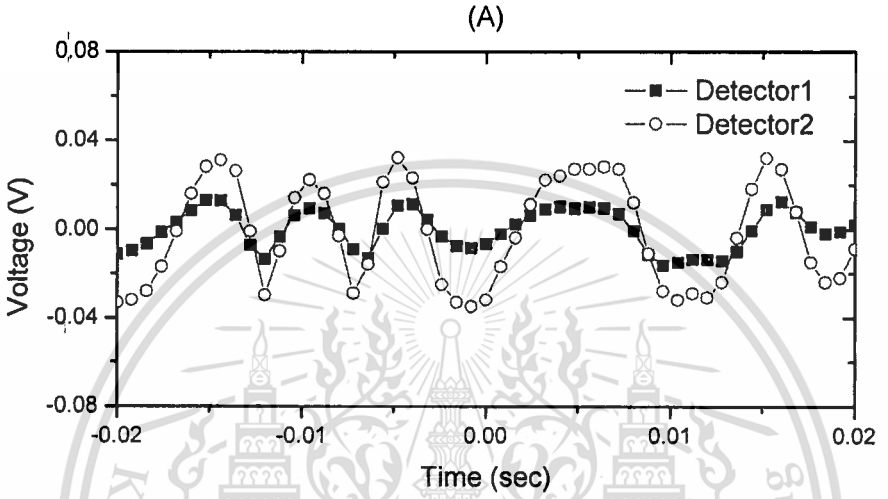

Figure 3.19 Interference signal of the experiment glass disk and object plane

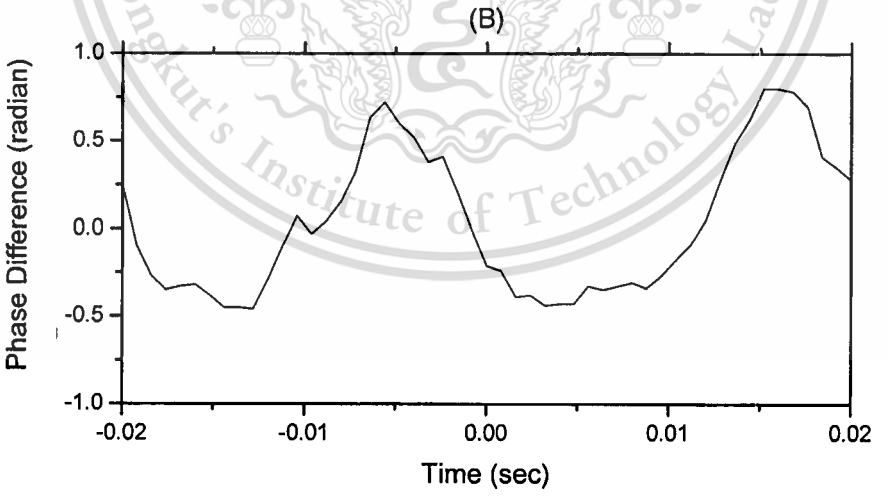

Figure 3.20 Phase calculation of the Hilbert transform for the one-dimensional phase distribution

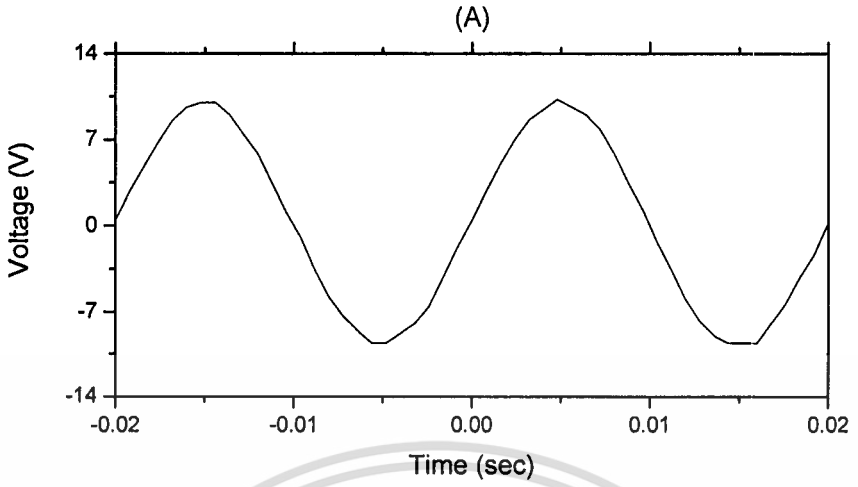

Figure 3.21 Input signal of piezoelectric actuator (@ 50Hz sine wave)

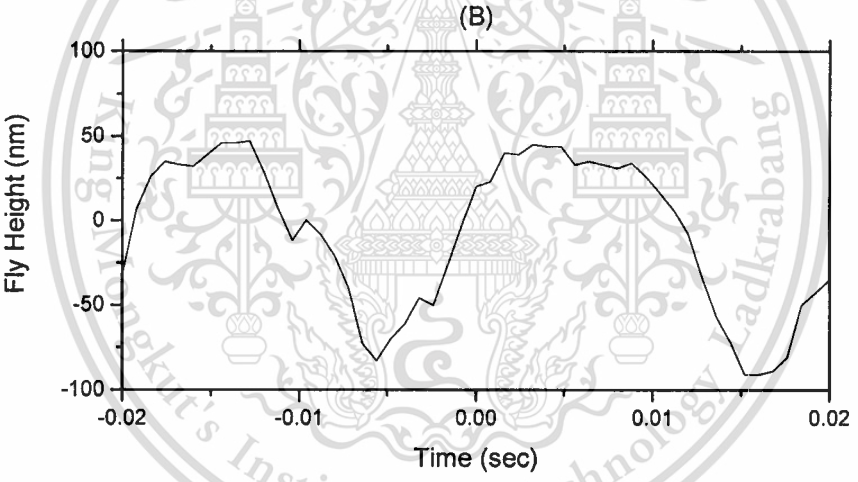

Figure 3.22 Fly height calculation result base on phase difference measurement method

From Figure 3.21 and 3.22, the input voltage (V) and flying height as function of period (T), the vertical axis of the graph shows the calculated flying height and the horizontal axis of the graph shows the period (T). Result indicated that input signals sent to piezoelectric actuator (PZT) is similar shape with calculated flying height. By the way, variation on calculated flying height curve might come from responsibility and sensitivity of the piezoelectric actuator.

Chapter 4

Conclusions

In this study of the phase difference measurement using a one-dimensional discrete Hilbert transform for application in the Fly height tester, these evaluates are separated for 2 parts; first of all, fly height measurement at initial state which measure only the surface of media glass disk (without object plane) and then install the object plan for measurement the fly height at experiment state. The proposed flying height measurement has been setwhich developed base on Dual-beam normal incidence polarization interferometry. The optical interferometry is used for capturing interference signal instead of interferometry receiver. The interference signal is captured and calculated by using a one-dimensional discrete Hilbert transform. Advantage of the proposed method is to simplify the flying height measurement set with maintain sensitivity of the system.

4.1 Fly Height Measurement at Initial state

The objectives for calculate phase difference and fly height at the initial state (without object plane) by measuring fly height only at the surface of media glass disk. The two measurement beams which reflecting at the 2 no coat surfaces of an experiment media glass disk are capture by high-speed optical detectors. Then use digital oscilloscope measuring the interference the signal from both detectors and record the result in text file format. The calculation is using Matlab program for calculate the phase difference per following procedure.

I. Calculate the reference fly height base on the phase difference (radian) for calculating the actual flying height from the experiment.

II. The 2 interference signals are captured in text file.

III. Use Hilbert transform to calculate the interference signal.

IV. Calculate phase referring to Trigonometric function

V. Calculate the phase difference by compare 2 phases together.

IV. Calculate the actual flying height by interpolate the phase difference result with the reference flying height

The result showed -0.08 radians phase difference and compute to distance at 8.02 nanometers which very close to zero. The corresponding normalized histogram tends to follow well a Gaussian distribution and standard deviation at 3 nanometers.

4.2 Fly Height Measurement at experiment state (with Object plane)

Objective of this evaluate for measurement and calculate a flying height of the experiment glass disk and objective plane (experiment slider). An evaluation separated into 2 parts follow by the input signals which are Triangular wave pulse and Sine Wave pulse.

4.2.1 Flying height measurement with Triangular wave signal

We applied Triangular wave pulse to piezoelectric actuator (frequency at 50 Hz and vary the amplitude from 5 to 20 volts) for varying the distance between experiment glass disk and slider. The interference signal is captured form both detectors use for calculate the actual flying height. Result indicated that input signals sent to piezoelectric actuator (PZT) is similar shape with calculated flying height. By the way, variation on calculated flying height curve might come from responsibility and sensitivity of the piezoelectric actuator.

4.2.2 Flying height measurement with Sine wave signal

For validating the system of phase measurement, we applied the Sine wave pulse to piezoelectric actuator (frequency 50 Hz and amplitude 5 volts) for varying the distance between experiment glass disk and slider. Actual flying height was calculated. Result indicated that input signals sent to piezoelectric actuator (PZT) is similar shape with calculated flying height. By the way, variation on calculated flying height curve might come from responsibility and sensitivity of the piezoelectric actuator.

Based on above results, we conclude that the phase difference measurement technique by using Phase comparison interferometry and One-dimensional discrete Hilbert transform was achieved in sub 10 nanometers spacing range. During experiment we observed that the deviation in measurement results caused by various random vibration from system and environment. For further improvement of this research we recommend consider on vibration, contamination, calibration and repeatability of the system.

References

[1] Peter de Groot et al. "Determining The Optical Constants of Read-Write Sliders During Flying-Height Testing" **APPLIED OPTICS.,** vol.37, no.22, August 1998.

[2] Xinqun Liu et al. "Normal Incidence Polarization Interferometer for Measuring Flying Height of Magnetic Heads" **IEEE TRANSACTIONS ON MAGNETICS.,** vol.35, no.5, September 1999.

[3] Christoph K et al. "Differential phase measurements in low-coherenceinterferometry without 2π ambiguity." **OPTICS LETTERS.,** vol.26, no.23, December 2001.

[4] Ribun ONODERAet al. "Interferometric Phase-Measurement Using a One-Dimensional Discrete Hilbert Transform." **OPTICAL REVIEW.,** vol.12, no.1, 2005. Pp.29-36

[5] Y. He et al. "Flying Height Measurement Based on Phase Comparison Michelson Interferometry Using White Light Illumination." **Manuscript Received.,** August 2006.

[6] Yinbo Heet al. "Fly Height Measurement Based on Phase Comparison Michelson Interferometry Using Low-Coherence Light Source." **IEEE TRANSACTIONS ON MAGNETICS.,** vol.44, no.2, February 2008.

[7] Mathias Johansson. "The Hilbert Transform" **Applied Mathematics.,** Pp. 22 – 25

[8] P. Hariharan **"Basic of Interferometry."** 2 nded, USA, Elsevier Inc, 2007.

Appendix

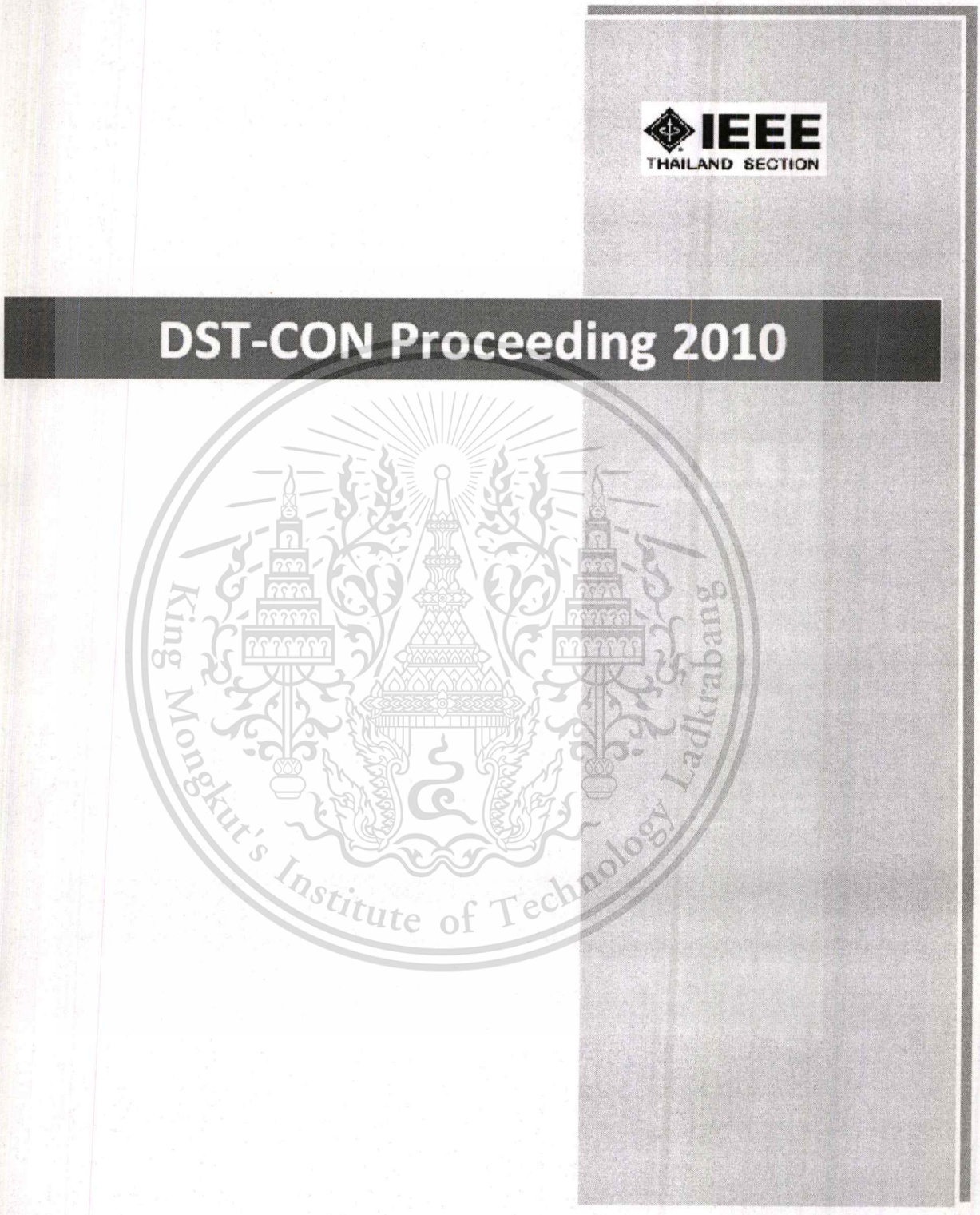

DST-CON 2010

Phase Difference Measurement Using a One-Dimensional Discrete Hilbert Transform for Application in Fly Height Tester

T Tanoi *), S Boonsang **),
*) College of Data Storage Technology and Applications, King Mongkut's Institute of Technology Ladkrabang, Bangkok 10520, Thailand
**) Electronics Department, Faculty of Engineering, King Mongkut's Institute of Technology, Ladkrabang, Bangkok 10520, Thailand

Abstract—**We present a method for measuring phase difference using a one-dimensional discrete Hilbert transform for application in fly height tester. The optical interferometry is used for capturing interference signal with separate to two orthogonal polarization states which represent to spacing range of each component. The captured signal and calculation results indicate that the propose method can be able to archive a resolution less than 1 nanometer.**

Keywords-Phase Difference Measurement; Hilbert Transform; One-Dimensional Discrete Hilbert Transform; Fly Height Tester

I. INTRODUCTION

Head flying height is the most effective critical parameters in hard disk drive (HDD). With increasing the recording density, head flying height has been minimized to nanometer scale. Currently, a high precision system employing interferometry technique has been used for testing this parameter. To date, there are many methods to measure a nanometer spacing range such as multiple wavelength interferometry (MWI) [1]. The multiple wavelength interferometry (MWI) has been implemented in the well-known dynamic flying height tester (DFHT) but, with a limitation of the dynamic flying height tester are on accuracy and calibration issue. To achieve the measurement of nanometer scale spacing phase base interferometry [1-4] has been introduced because of their high sensitivity and rebut at any spacing range.

In our present study, we proposed a method to measure phase difference by using optical interferometry [3] as shown in figure 1 and calculate amplitude and phase information by a one-dimension discrete Hilbert transform [2].

II. EXPERIMENT SETUP

The phase difference measurement system is shown in figure 1. A laser source is a Helium Neon laser with an emitting wavelength 632.8 nm at maximum 0.5 mW. A polarizer (Linear Polarizer, VIS 550 – 1500 nm) orients at 45o is used to separate the laser light into two polarization states.

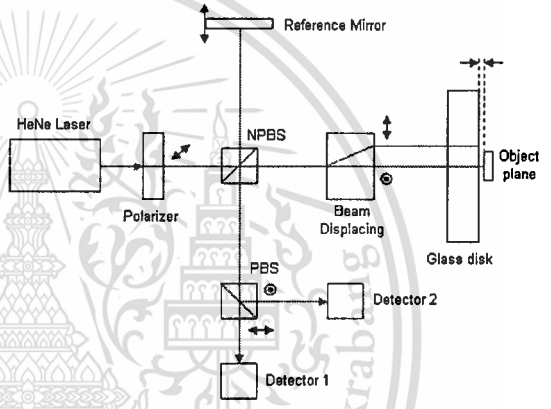

Figure 1. Sketch of the instrument in measurement state: NPBS, non-polarizing beam splitter; PBS, polarizing beam splitter.

A non-polarizing beam splitter is split the beam to reference mirror as reference beam and a sample beam. The reference beam is use for providing the equal reference power for horizontally and vertically polarized light. The sample beam passes through the beam displacing which splits the parallel beam into the experiment disk (3.5 inch diameter quartz disk with the 3 mm thickness and the top surface is coated with anti-reflective material) and object plane. The two beams are reflected at the difference components and travel back through beam displacing and non-polarizing beam splitter. At the non-polarizing beam splitter, all beams are combining and interface with each other. The polarizing beam splitter is split all beam into two orthogonal polarization states which represent to each component, and detect the interference signal by the high-speed optical detectors.

III. RESULT AND DISCUSSION

In our experiment, we captured the interference signals for 2 states, initial state which is no objective plane (to simulate the head) and measurement state by adding object.

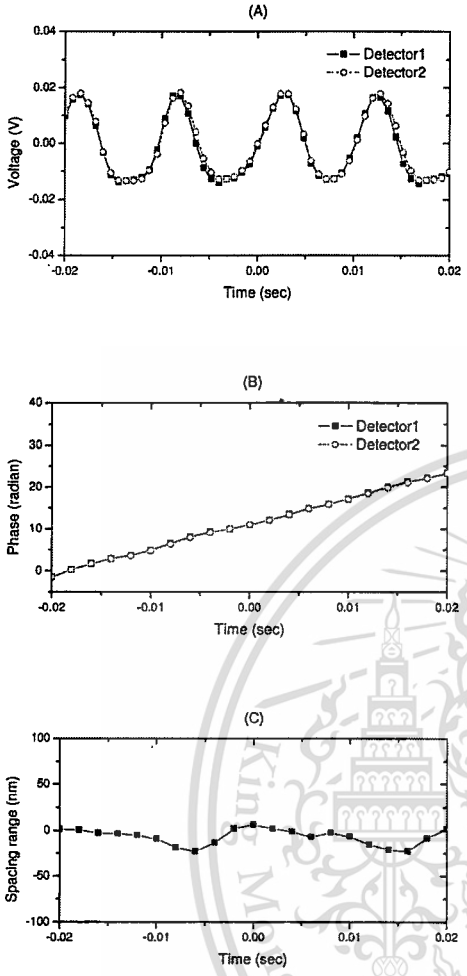

Figure 2. Calculation result of the One-dimensional discrete Hilbert transform for interference signal at initial state (without object plane); (A) Interference signal of the experiment glass disk, (B) Phase calculation of the Hilbert transform for the one-dimensional phase distribution. (C) Spacing range of experiment glass disk and object plane.

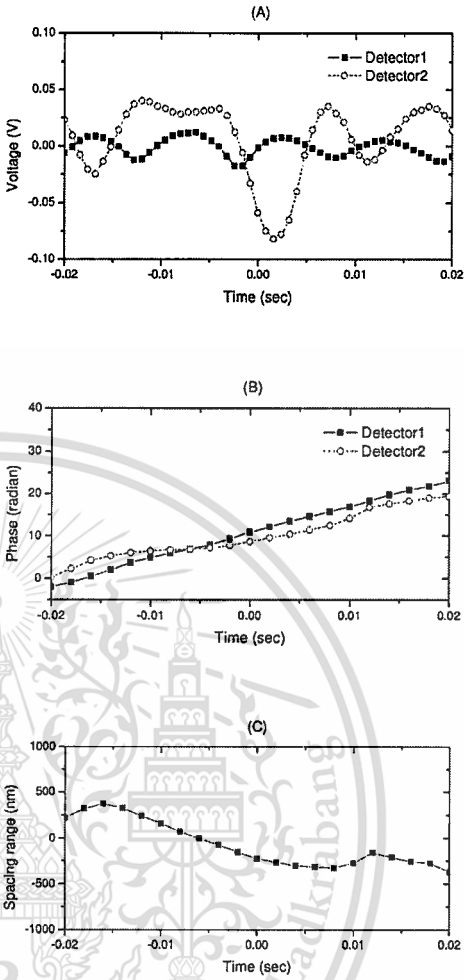

Figure 3. Calculation result for interference signal at measurement state; (A) Interference signal of the experiment glass disk (blue curve) and the object plane (red curve), (B) Phase calculation of the Hilbert transform for the one-dimensional phase distribution. (C) Spacing range of experiment glass disk and object plane.

Figure 2 shows the experimental and calculated results for initial state (without object plane). The interference signals that reflected from experiment glass disk and combining with reference beam as shown in figure 2(A), solid and dash curves represent the interference signal from detector1 and detector2 respectively. Figure 2(B) shows the calculation of One-dimensional discrete Hilbert transform and phase distribution (in radians), the result show -0.08 radians phase difference and compute to spacing range is 8.02 nanometers which very close to zero as shown in figure 2(C).

Figure 3 shows the experimental and calculated results when the object is closed to the glass disk. The calculation result shows phase difference at -0.67 radians, 67.92 nanometers spacing range has presented in figure 3(C).

Based on experiment results, we conclude that the propose instrument was archived a spacing range in sub 100 nanometer. However, during experiment we observed that the deviation in measurement results caused by various random vibration from system and environment. For further improvement of this paper we recommend consider on vibration, calibration and repeatability of the system.

IV. Conclusion

We have developed a phase difference measurement technique by using Phase comparison interferometry and One-dimensional discrete Hilbert transform. The numerical calculation of the interference signals, phase distribution and distance of glass disk and object place in sub 100 nanometer spacing range has been presented. In

our experiment, we observe that the deviation which caused by various random vibration. For the further improvement, the measurement could be eliminated the various random vibration by improving the vibration absorption system.

ACKNOWLEDGMENT

This paper is supported from Industry/University Cooperative Research Center in Data storage Technology and Applications, King Mongkut's Institute of Technology Ladkrabang and National Electronics and Computer Technology Center, National Science and Technology Development Agency and Western Digital (Thailand) Co., Ltd.

REFERENCES

[1] Y. He, H. Zhang, K. Fukuzawa, and Y. Mitsuya, "Fly Height Measurement Based on Phase Comparison Michelson Interferometry Using Low-Coherence Light Source", IEEE, vol. 44, pp. 309-314, 2008.

[2] R. ONODERA, H. WATANABE and Y. ISHII, "Interferometric Phase-Measurement Using a One-Dimensional Discrete Hilbert Transform", Optical review, Vol. 12, pp. 29-36, 2005.

[3] C. K. Hitzenberger, M. Sticker, R Leitgeb, and A. F. Fercherand, Opt. Lett. 26, 1864 (2001).

[4] C. K. Hitzenberger and A. F. Fercher, Opt. Lett. 24, 622 (1999).

Author Biography

Name	Mr.Tepparit Tanoi
Birthday	November 22, 1979
Address	35 M. 5 Tambon Kudsra, Amphoe Muang, Udonthani 41000
	Tepparit.Tanoi@gmail.com
	Tepparit.Tanoi@wdc.com
Education	2002, Graduated in Bachelor of Science in Industrial Education of King Mongkut's Institute of Technology Ladkrabang.
	2011 (Present), Master degree of Engineering in college of Data Storage Technology and Application of King Mongkut's Institute of Technology Ladkrabang.
Published research	"Phase Difference Measurement Using a One-Dimensional Discrete Hilbert Transform for Application in Fly Height Tester", the 3rd International Data Storage Technology Conference 2010 (DST-CON2010) on 30 Jul - 1Aug 2010, Bangkok, Thailand.